Transportmetrica A: Transport Science

ISSN: 2324-9935 (Print) 2324-9943 (Online) Journal homepage: www.tandfonline.com/journals/ttra21

Conflict detection and resolution for distance-to-go railway signalling

Nina D. Versluis, Paola Pellegrini, Egidio Quaglietta, Rob M.P. Goverde & Joaquin Rodriguez

To cite this article: Nina D. Versluis, Paola Pellegrini, Egidio Quaglietta, Rob M.P. Goverde & Joaquin Rodriguez (08 Dec 2025): Conflict detection and resolution for distance-to-go railway signalling, Transportmetrica A: Transport Science, DOI: 10.1080/23249935.2025.2592225

To link to this article: https://doi.org/10.1080/23249935.2025.2592225

Published online: 08 Dec 2025.

TRANSPORTMETRICA A: TRANSPORT SCIENCE
https://doi.org/10.1080/23249935.2025.2592225

Taylor & Francis
Taylor & Francis Group

Conflict detection and resolution for distance-to-go railway signalling

Nina D. Versluis [a], Paola Pellegrini [b], Egidio Quaglietta [a], Rob M.P. Goverde [a] and Joaquin Rodriguez [b]

[a]Department of Transport and Planning, Delft University of Technology, Delft, The Netherlands ;
[b]COSYS-ESTAS, Université Gustave Eiffel, Villeneuve d'Ascq, France

ABSTRACT

Conflict detection and resolution models typically consider train separation distances based on a number of blocks corresponding to conventional fixed-block signalling systems. However, modern distance-to-go railway signalling systems, such as the European Train Control System (ETCS), use braking curve supervision, resulting in train- and speed-dependent train separation distances. This paper proposes a modelling approach that incorporates train- and speed-dependent brake indication points and the resulting blocking times, enhancing conflict detection and resolution models for distance-to-go signalling. By integrating these enhancements into the state-of-the-art RECIFE-MILP model, a mixed integer linear programming formulation explicitly representing fixed-block distance-to-go signalling is obtained. The enhanced model is evaluated considering the state-of-practice fixed-block distance-to-go signalling system ETCS Level 2, and is compared with the original model for conventional fixed-block signalling in two real-world case studies. Results show that the shorter train separation under distance-to-go signalling leads to different rescheduling decisions, including a significant number of reroutings and some reorderings. With that, reductions in total train delay are achieved for 98% and 55% of the respective case study instances. While the mean reductions are below 1%, reductions of up to 7% are observed. These findings illustrate the operational relevance of incorporating distance-to-go principles into conflict detection and resolution modelling.

ARTICLE HISTORY
Received 31 January 2025
Accepted 14 November 2025

KEYWORDS
Railway traffic management; rescheduling; ETCS level 2; mixed integer linear programming

1. Introduction

Worldwide, railways are experiencing a continuously increasing travel demand. The existing railway networks have limited capacity and fewer and fewer extension possibilities due to the costly and land-consuming infrastructure. Especially at capacity bottlenecks such as in and around stations, extensions are often not available. To fulfil future railway demand

CONTACT Nina D. Versluis n.d.versluis@tudelft.nl Department of Transport and Planning, Delft University of Technology, Stevinweg 1, 2628 CN Delft, The Netherlands

in a different way, advanced signalling systems such as distance-to-go (DTG) systems are developed as capacity-increasing alternatives to conventional fixed-block multi-aspect signalling with automatic train protection systems.

In conventional fixed-block systems, the track is partitioned into blocks of fixed lengths which can be occupied by at most one train at a time. The block entries are protected by trackside multi-aspect signals which indicate whether an approaching train can proceed, needs to start braking or is required to stop. The automatic train protection system supervises that the trains follow the signal aspects and intervenes when a train does not start braking after a brake indication. Hence, train separation distances are determined based on a number of blocks of fixed length.

Fixed-block DTG systems feature radio-based cab signalling and continuous braking curve supervision from the train front position to the block (or section) entry corresponding to the train's end of movement authority (MA), i.e. the permission to move to a specific location under supervision. With this, brake indications no longer need to be provided at the entry of a block. Moreover, train separation distances become speed-dependent due to the approach distance to the first occupied block being based on the train's absolute braking distance.

For effective railway operations, real-time traffic management is crucial. In case of small delays originating from variations in rolling stock, dwell times and driver behaviour, traffic management can apply rescheduling measures such as retiming, reordering and local rerouting to resolve track conflicts while minimising the delay propagation in the network. To support human dispatchers in taking mathematically optimised rescheduling decisions, conflict detection and resolution (CDR) models describing variants of the real-time railway traffic management or rescheduling problem are developed (Cacchiani et al. 2014; Pellegrini, Marlière, and Rodriguez 2014). In short, the problem can be formally described as follows: given a railway network and timetable together with delayed events, find a new timetable by rescheduling trains such that all track conflicts are resolved and total delay (or other relevant objective) is minimised.

The existing CDR models mostly refer to conventional fixed-block signalling systems. As a result, they are typically microscopic models that inherently rely on the discretisation of the track into fixed blocks. Moreover, they generally neglect changes in the speed profile to fit the adjusted timetable (Reynolds and Maher 2022). Hence, these models cannot accurately capture the speed-dependent separation distances typical for DTG signalling due to the implementation of braking curve supervision (Versluis et al. 2024).

In this paper, we address the research gap regarding CDR for DTG signalling by developing a CDR model for DTG and applying it to assess the operational relevance of modelling CDR for DTG. To obtain a model that represents and identifies optimised rescheduling decisions for DTG railway operations, we propose enhancements for existing CDR models. The enhancements include the introduction of speed profile options and train blocking times considering train- and speed-dependent braking distances. These two enhancements are significant as they are crucial in enabling the modelling of train- and speed-dependent brake indication points in CDR models. As a proof of concept, we incorporate the enhancements into the state-of-the-art CDR model of RECIFE-MILP (Pellegrini et al. 2015), together with a distinction between switches and the rest of the track. The resulting model is assessed through a comparative analysis with the original one for conventional fixed-block

signalling in two case studies, specifically in terms of total train delay and rescheduling decisions.

With this, the main contributions of the paper are:

- A modelling approach for enhancing conflict detection and resolution models to apply to distance-to-go signalling, introducing train- and speed-dependent train separation and brake indication points.
- A mixed-integer linear programming model for conflict detection and resolution under distance-to-go signalling, obtained by integrating distance-to-go principles into the state-of-the-art RECIFE-MILP model.
- A comparative analysis illustrating the operational relevance of incorporating distance-to-go principles into conflict detection and resolution modelling, as different rescheduling decisions achieving reductions in total train delay are proposed.

The paper is organised as follows. In Section 2, the state-of-the-art related to the modelling of CDR for DTG signalling is provided. Section 3 describes the enhancement approach for CDR models to describe DTG signalling. The mathematical formulation of the fixed-block CDR model RECIFE-MILP enhanced for DTG signalling is presented in Section 4. Section 5 presents the results of the comparative analysis. Finally, Section 6 concludes the paper.

2. State-of-the-art in conflict detection and resolution for distance-to-go signalling

In this section, we provide an overview of the state-of-the-art relevant for the topic of modelling CDR under DTG signalling. Section 2.1 focuses on DTG signalling as the de-facto standard in the development of next-generation signalling systems. Section 2.2 provides an overview on modelling approaches for CDR existing in the literature.

2.1. Distance-to-go signalling systems

In the development of next-generation signalling systems, DTG is the de-facto standard. For the mainline railways, DTG signalling is included within the European Train Control System (ETCS) and the Chinese Train Control System (CTCS). For metro lines, Communication-Based Train Control (CBTC) applies DTG signalling principles. Examples of deployed DTG systems are the fixed-block ETCS Level 2 with Trackside Train Detection (TTD) and the similar CTCS Level 3. The latter is designed for the Chinese high-speed (up to 300 km/h) railway lines (Xu et al. 2017). In this paper, we focus on ETCS Level 2 with TTD, hereafter referred to as ETCS L2, which is implemented on freight and passenger railways throughout the world (European Rail Supply Industry Association 2022).

To enable cab signalling, ETCS L2 features radio communication between a radio block centre on the trackside and the trains as follows. The radio block centre receives train position information from a train. This information supports the request for a route extension to the interlocking system. Based on safety logic and input from TTD, the interlocking system sets and locks a new route for the train. As a next step, the radio block centre updates the MA before sending it to the train. With the received MA, the train recomputes and supervises a dynamic speed profile including continuous braking curves.

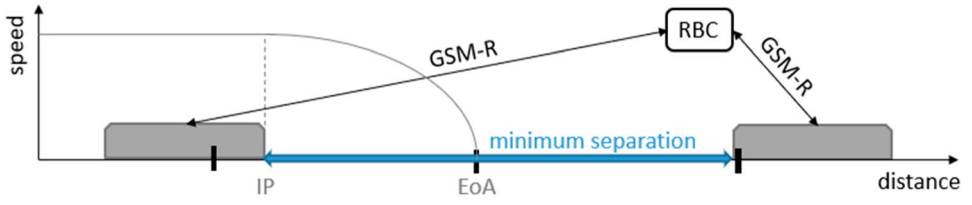

Figure 1. Schematic layout of the minimum separation between two trains in a speed-distance diagram under ETCS L2 with (block) section boundaries, radio block centre (RBC) and radio communication (GSM-R). The separation is related to the brake indication point (IP) and the end of authority (EoA) depending on the braking curve.

Corresponding to the braking curves, the brake indication point for a train can lie anywhere along the track. The end of authority, however, is consistently set at the end of a block or TTD section (TDS). The TDSs correspond to the parts of the track in which the presence of a train is automatically detected. Whether the end of authority corresponds to a block or TDS depends on the implemented ETCS L2 variant. It can also depend on whether it is on the open line, in a station or around switches. A schematic representation of the ETCS L2 system is provided in Figure 1. In the figure, two trains at the speed-dependent minimum separation distance are included.

Within ETCS and CTCS, more advanced application levels are being developed, but not yet deployed. In particular, ETCS Level 2 with onboard train integrity monitoring (TIM), previously known as ETCS Level 3. This allows the end of authority to be located at the end of the last free virtual (non-physical) block, e.g. in ETCS Level 2 Virtual Block, or even at a safety margin behind the rear position of a moving train, e.g. in ETCS Level 2 Moving Block (European Railway Agency 2016).

2.2. Conflict detection and resolution modelling

Based on the DTG signalling principles as described in Section 2.1, three interesting aspects for CDR models are the infrastructure representation, the assumption related to speed and the modelling of train separations (Versluis et al. 2024). In the context of CDR, the infrastructure is typically modelled at the microscopic level (Cacchiani et al. 2014), which allows the use of the well-known blocking time theory (see, e.g, Hansen and Pachl 2014) in the modelling of train separation. The alternatives of mesoscopic and macroscopic approaches are more often considered in case of disruptions rather than disturbances (Cacchiani et al. 2014; Zhan et al. 2022).

In this section, we provide an overview of the existing models and methods, to further specify the gap in the modelling of conflict detection and resolution for distance-to-go railway operations. Section 2.2.1 focusses on the main types of model formulations in the literature. In Section 2.2.2, solution methods are discussed in the light of practical applicability. Table 1 provides a summary of the reviewed literature aimed at comparing the work presented in this paper with the key existing works. We specifically consider the following features: whether the infrastructure is modelled in terms of blocks or TDSs, how speed is modelled, whether and how speed is considered in the train separation distance, which rescheduling decisions are considered, which solution method is applied, what model objective is considered, and to what kind of scenario is it applied.

Table 1. Comparison of this work with related works on key features in conflict detection and resolution modelling.

Work	Infra modelling	Speed modelling	Speed in sep. dist.	Rescheduling decisions	Solution method	Model objective	Application scenario
D'Ariano, Pranzo, and Hansen (2007)	Blocks	Iterative	No	RT,RO	B&B	Max secondary	20-km area
Lamorgese and Mannino (2015)	Blocks	Fixed	Fixed	RT,RO,RR	Macro/micro decomposition	Mean station	100-km lines delay cost
Luan et al. (2018)	Blocks	Multiple profiles	Yes	RT,RO,RR	Two-level	Total mean	50-km corridor station delay
Mazzarello and Ottiviani (2007)	Blocks	Iterative	No	RT,RO,RR	Two-level	Max secondary	44-km area
Pellegrini et al. (2015)	TDSs	Fixed	No	RT,RO,RR	Heuristic	Total final delay	Various control areas
Reynolds and Maher (2022)	TDSs	Two profiles	No	RT,RO,RR	B& P	Custom utility	Ext. station area
Törnquist and Persson (2007)	Blocks	Fixed	No	RT,RO	Solver	Total delay	400-km network
Xu et al. (2017)	Blocks	Multiple levels	Yes	RT,RO	Two-step	Total secondary delay	high-speed corridor like network
This work	TDSs	Two profiles	Yes	RT,RO,RR	Two-step solver	Total delay, amx speed penalty	17-km junction, 68-km corridor

sep. dist.: train separation distance, TDSs: trackside train detection section, B&B: branch-and-bound, B&P: branch-and-price, RT: retiming, RO: reordering, RR: rerouting, Max: maximum.

For a more extensive review of the existing literature on CDR models in the context of DTG signalling, we refer to Versluis et al. (2024).

2.2.1. Models

Three main model classes can be defined: alternative graph, disjunctive (or big-M) mixed integer linear programming (MILP) and time-indexed MILP models.

The main benefit of formulating the CDR problem as an alternative graph is the relation with general scheduling problems for which proven solution algorithms exist (D'Ariano, Pacciarelli, and Pranzo 2007; Marcis and Pacciarelli 2007; Mazzarello and Ottiviani 2007). Alternative graph models typically rely on a microscopic representation of the infrastructure, assuming an infrastructure discretisation corresponding to the fixed-block signalling system. However, the specific formulation also limits the flexibility of the resulting models. For example, as an objective function only the minimisation of the maximum secondary delay can be considered. Also, the initial formulation does consider train occupation times in the separation modelling, rather than the full blocking times. This is however shown to be surmountable by explicitly adding the approach time component (Corman et al. 2009). Other downsides are the serious difficulties in the inclusion of rerouting and speed beyond the fixed-speed assumption. Some efforts have been made concerning both (D'Ariano et al. 2008; Mazzarello and Ottiviani 2007). The fixed-speed CDR model can be used in an iterative scheme with a speed profile generation model to find a valid speed profile for a computed rescheduling solution (D'Ariano, Pranzo, and Hansen 2007; Mazzarello and Ottiviani 2007). The model of D'Ariano, Pacciarelli, and Pranzo (2007) is considered in the application to moving-block signalling by Janssens (2022). Unsurprisingly, model restrictions in terms of objective, rerouting, speed, and train separation resonate throughout this early-stage moving-block research (Versluis et al. 2024).

In disjunctive MILP CDR models, by which we mean MILP models with disjunctive constraints representing 'or' conditions, railway operations are described by decision variables and mixed integer linear constraints, complemented with a linear objective function (Luan et al. 2018; Pellegrini et al. 2015; Törnquist and Persson 2007; Xu et al. 2017). Though linearity of a model is generally desirable, there is also a downside to it. To obtain linear constraints, the approach relies on the big-M linearisation method (Bazaraa, Jarvis, and Sherali 2008). The drawback of that method is that it is a weak linearisation, which makes the resulting model hard to solve to optimality (Reynolds et al. 2020). The formulation is flexible in terms of model objectives and rescheduling, including rerouting. It is also fairly flexible in terms of infrastructure, speed, and separation modelling, though some remarks are needed here (Versluis et al. 2024). First, some form of discretisation is required for the infrastructure. Second, fixed-speed assumptions based on one speed profile are most common. However, Luan et al. (2018) and Xu et al. (2017) considered speed levels in their applications to fixed-block and distance-to-go signalling, respectively. Immediately, train separation times become speed-dependent through the consideration of full blocking times. The latter is typical in disjunctive MILP models, though Törnquist and Persson (2007) instead assume fixed train separation times.

Known for their strong linearisation and good approximation for scheduling problems (Van den Akker, Hurkens, and Savelsbergh 2000), time-indexed MILP models are considered as an alternative to disjunctive MILP formulations for the CDR problem (Bettinelli, Santini,

and Vigo 2017; Lusby et al. 2013; Reynolds et al. 2020). The models feature resources that correspond to pairs of a time unit and a track part. Possible train routes can be visualised as sink-source paths in a time-space graph corresponding to the problem instance. This makes the time-indexed approach generally well-suited for the consideration of rerouting (Bettinelli, Santini, and Vigo 2017; Lusby et al. 2013; Reynolds et al. 2020). These resources, however, seriously limit the model's application possibilities. The necessary discretisation of time and space restricts the flexibility in the modelling of running and separation times, and capacity, respectively. It is also the cause of the main drawback of the approach, i.e. the model size (Reynolds et al. 2020; Van den Akker, Hurkens, and Savelsbergh 2000). Lusby et al. (2013) and Reynolds and Maher (2022) model speed beyond fixed-speed assumptions. They consider alternative speed profiles corresponding either to running at a constant speed or to accelerate/decelerate around a stop.

From this overview, we conclude that DTG signalling is underrepresented within the variety of CDR models, especially in the context of mainline railways. Besides the model formulation, important limitations of existing models are the dependencies on the infrastructure discretisation and the incorporation of speed in train separation modelling. In this paper, we contribute to the challenge of making CDR models more applicable for DTG signalling by addressing both infrastructure and speed modelling. Our goal is to model train separation based on full blocking times taking into account absolute braking distances, with a focus on the mainline railways, in order to assess the operational relevance of DTG signalling in CDR.

2.2.2. Solution methods and practical applications

Given the above overview of the main type of models, the next step is to look at the solution methods considered in literature. The solution approach is of great importance for the practical applicability of CDR models due to the real-time nature of the modelled problem. Hence, the focus here is on approaches that have an impact on computation times.

Traditionally, solving MILP models involves branch-and-bound algorithms, which are also implemented in commercial solvers such as CPLEX. Branch-and-bound is an exact method but can be enhanced by heuristic techniques to speed up the solution process. Examples applied to CDR are the truncated branch-and-bound algorithm proposed by D'Ariano, Pacciarelli, and Pranzo (2007) or the tailored branch-and-price algorithm of Reynolds et al. (2020). Also, iterative (meta)heuristics are considered in literature to obtain rescheduling solutions within effective computation times (Zhang et al. 2024).

As alternative solution approaches to tackle the challenge of finding good solutions quickly, exact decomposition methods are considered, e.g. by Lamorgese and Mannino (2015) and Leutwiler and Corman (2022). Lamorgese and Mannino (2015) introduce an exact macro-/microscopic decomposition of the CDR problem, inspired by the Bender's decomposition approach. The resulting iterative process of solving the problem at a macroscopic level and searching for feasible train routes through stations, has been applied in pilot tests in practice. Leutwiler and Corman (2022) apply a logic-based Benders decomposition, in which the subproblem is the feasibility counterpart of the master optimisation problem. Applied on a case study from the Swiss Federal Railways (SBB), the presented approach is up to 40 times faster than the centralised approach combined with a commercial solver.

Several other decomposition methods are considered in literature, which can, e.g. be found in the review papers of Leutwiler and Corman (2023) and Marcelli and Pellegrini (2021). Here, we mention two works that are based on the earlier mentioned MILP formulations of Törnquist and Persson (2007) and Pellegrini et al. (2015), respectively. Lippes (2024) and Yi et al. (2023) both propose an iterative approach based on a geographical decomposition of the network and a coordination algorithm to combine the local rescheduling solutions into an overall feasible solution. Per iteration, Lippes (2024) obtains a (moving-block) rescheduling solution for one subarea, while Yi et al. (2023) obtains (fixed-block) rescheduling solutions for all subareas separately. Both non-exact methods lead to significant computation time reduction compared to the centralised counterpart in most scenarios.

On a different note, model predictive control (MPC) is proposed as alternative modelling approach for the CDR problem by, e.g. Caimi et al. (2012) and Pochet, Baro, and Sandou (2016). Caimi et al. (2012) propose an MPC approach for rescheduling within complex central station areas, incorporating the retiming and rerouting of trains as well as partial speed profile coordination. With an SBB case study, it was demonstrated that this approach is viable for practical applications. Pochet, Baro, and Sandou (2016) apply an MPC-based approach in the context of suburban railway lines with mixed CBTC traffic, considering retiming and reordering measures. The approach is incorporated in a microscopic simulation tool of the French train operator SNCF.

In general, actual real-life implementation of CDR in traffic management systems are rare. Lamorgese et al. (2018) mention a few, of which here we report the ones with supporting documentation. Well-represented here is Bombardier Transportation (acquired by Alstom in 2021), with an optimisation-based support system (temporary) embedded in the traffic management system of some terminal stations of the Milano Undergound (Mannino and Mascis 2009), on various main lines in Italy (Mannino 2011) and Latvia. In the Milano system, an exact branch-and-bound was used as solution algorithm. In the later two, the stricter business rules required a heuristic approach, with which computational speed was gained with minimal loss in the 'optimal' performance. As already shortly referred to, the exact decomposition method of Lamorgese and Mannino (2015) has been applied on a Norway railway line with the involvement of the local infrastructure manager and train operating companies.

Overall it is clear that for practical applications, the straightforward MILP solving methods are unlikely to be sufficient. We note that practical application is not a focus point in this paper, but we acknowledge the importance of it and the related real-time performance. Specifically, when evaluating the model's performance and in following steps.

3. Distance-to-go signalling in conflict detection and resolution models

In this section, we present our approach for enhancing microscopic fixed-block CDR models to describe DTG signalling. The proposed enhancements focus on capturing the characteristics of train separation under DTG signalling. As observed, the dependence of train separation on speed and infrastructure discretisation touches upon gaps in the CDR literature. For an accurate modelling of the continuous relation between speed and train separation under braking curve supervision, we need to relax the (fixed-block) discretisation of the infrastructure and the fixed-speed assumptions. This allows for the incorporation

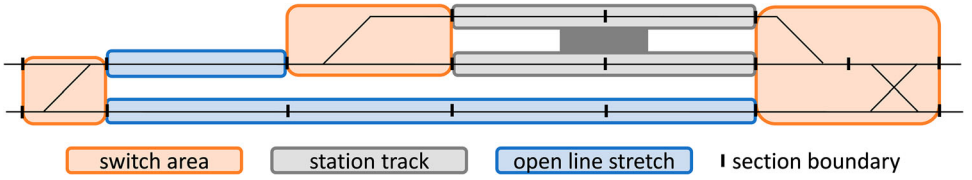

Figure 2. Infrastructure divided into switch areas, station tracks and open line stretches.

of (train- and) speed-dependent brake indication points. Along that line, we address the following three aspects: (1) switch and track areas, (2) speed profile options, and (3) blocking times for DTG signalling.

3.1. Switch and track areas

The discretisation of the track can be different around switches and on the (rest of the) track. To accommodate the resulting differences in DTG blocking times, we divide the infrastructure into switch areas and tracks, as commonly considered in the field. A switch area contains a collection of sections, e.g. TDSs or (virtual) blocks, such that it has more than two entry and/or exit points. Depending on the track layout, i.e. the relative closeness of switches, a switch area can contain one or more switches. In practice, two switch areas should lie more than the maximum passable train length apart. This allows all trains to come to a standstill between the switches without blocking traffic over either of them. Two switch areas are connected by one or more tracks. We distinguish two types of tracks: station tracks and open line stretches. If a track lies at a station, it is a station track. If not, the track is an open line stretch. Parallel tracks connecting two switch areas are considered as separate station tracks and/or open line stretches. Figure 2 illustrates the division of the infrastructure into switch areas, station tracks and open line stretches.

We propose a discretisation of the track beyond the fixed-block structure. The discretisation can correspond to physical blocks, TDSs or virtual blocks. We introduce the concept of locations to indicate the discretisation points corresponding to section entry points. In the rest of the paper, when suitable, locations in switch areas are distinguished from locations on the tracks, by referring to them as *switch locations* and *track locations*, respectively. This distinction enables the modelling of possibly different blocking times in switch areas and on the track. For example, by reserving switch locations within a switch area together and track locations independently from one another.

3.2. Speed profile options

Consistent with the speed dependency of train separation under DTG signalling, the notion of speed modelling is extended to two speed profile options. That is, the option to run according to the *maximum speed profile* and the option to run according to a *scheduled speed profile*. In general, maximum speed profiles are characterised by maximum acceleration, a target cruising speed equal to the maximum speed and maximum deceleration, and scheduled speed profiles by a lower target cruising speed and, possibly, coasting phases. Figure 3 shows examples of a maximum and a scheduled speed profile between two stops, considering an intermediate track speed restriction.

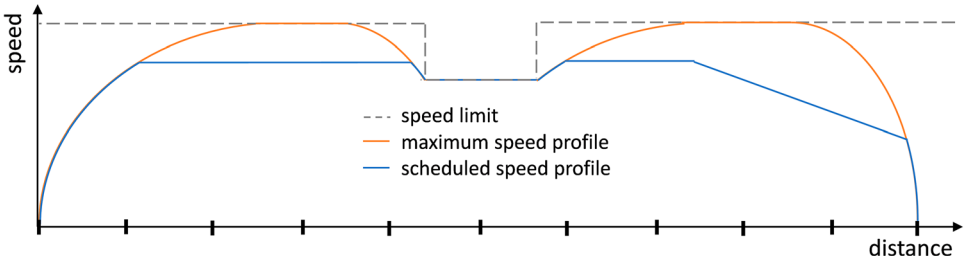

Figure 3. Maximum and scheduled speed profile between two stops with a speed restriction.

We propose to consider speed profiles only on the track, i.e. on open lines and station tracks. Within switch areas, speed is typically restricted and track occupation times should be kept to a minimum. Hence, we assume unique train running times in switch areas, independently of the speed profile assigned before or after. We consider the speed profile to not change on a track, but different profiles can be used on different tracks by a train. Hence, trains can only transition between speed profiles in switch areas, where the speed is limited and assumed to be the same. This may significantly reduce the size of the model compared to allowing changes at every location separately. For every track, the first location is selected as *speed assignment location*. Only at these locations, speed profiles are assigned (one for each train along each route).

The introduction of speed profile options affects the train running and clearing times. The minimum running and clearing times corresponding to the maximum speed profile are taken as reference. For cases in which trains are operating according to the scheduled speed profile, the longer running and clearing times with respect to the minimum times can be predetermined and included as input parameters.

Typically, scheduled speed profiles are assigned. Trains should only run according to the maximum speed profile if the situation requires it. For example, maximum speed profiles can be followed if the train is delayed or when it can reduce the impact of a delayed train. To encourage the assignment of scheduled speed profiles, the minimisation of the number of maximum speed profile assignments can be included in the model objective.

We note that despite the introduction of a second speed profile option, the enhanced model will still be a fixed-speed model. Also in case of considering more than two speed profile options, this notion will remain to a certain extent. In this work, we have opted for two speed profile options as a compromise between the computational efficiency, which is negatively affected by more speed profiles options through the increasing model size, and realism, which is positively affected by more speed profiles that increases the model accuracy. This trade-off is based on the matter that CDR models are not actually representing railway operations itself, as opposed to, for example, simulation models.

3.3. Blocking times for distance-to-go signalling

With their direct relation to minimum train separation, blocking times are the core of microscopic CDR models. In the blocking time components, DTG principles are incorporated to describe the minimum train separation based on speed-dependent braking distances.

The minimum separation between a pair of trains at a specific location can be expressed in terms of their blocking time components. Related to the leading train, we need to take

into account the train's clearing and release time of the section starting at the location. Concerning the following train, we need to consider its setup, reaction and approach time related to that location. Due to locations referring to fixed discrete points, we should also include the leading train's running time from one location to the next.

The train- and speed-dependency of the separation distance is clearly presented in the approach time, i.e. the time it takes to cross the approach distance. The DTG approach distance is defined as the braking distance supplemented with a safety margin. The inclusion of a safety margin accounts for the uncertainties in train position and speed due to, for example, measurements errors. To be able to describe this in the model, we introduce the concept of *reference (brake) location*. For track locations, reference locations are set to lie minimally the approach distance before the location's position on the track. For switch locations, reference locations are obtained similarly, but always considering the previous location in the switch area along a specific route.

In the following, we formalise the DTG approach distance based on its definition in terms of braking distance and safety margin. For a given combination of train, location and (approaching) speed, the DTG approach distance can be determined as follows Brünger and Dahlhaus (2014):

$$\text{approach distance} = \frac{\text{speed}^2}{2\,(\text{braking rate} + \text{resistance deceleration})} + \text{safety margin}, \quad (1)$$

with the approach distance and safety margin in metres, the speed in metres per second, and the braking rate and resistance deceleration in metres per square second^2. For a correctly defined approach distance, we assume the braking rate to be constant. That is, for a certain train and speed, we assume one braking rate that best approximates the train's braking curve up to the given speed. The deceleration due to the resistance of the train on the track depends on the train, the speed of the train at the location and the track gradient at the location, and can be, e.g. expressed according to a quadratic equation of speed (Davis 1926).

We note that our definition of braking distance differs from the ones that are based on the ETCS braking curve computations of the European Railway Agency (2020). The main difference is that we consider the distance traversed by the train from the moment the brakes start to work, i.e. the braking point, while the European Railway Agency (2020) considers the distance traversed by the train from the moment a brake indication, i.e. at the indication point, is issued by the system. The (travelling) time between the indication and braking points can be described as the human and system reaction times, which is modelled in the blocking time component 'reaction time'.

Given a location, train and speed, the approach distance formula provides the braking point before the location. As illustrated in Figure 4, this point may not coincide with a modelled discrete track location: the last track location before the braking point is defined to be the reference (brake) location. Hence, the reference location lies some lag distance earlier along the track than the braking point. Note that the lag distance is strictly shorter than the length of the track between the reference location and its succeeding location, i.e. the entry point of the next section along the train's route. This length is also referred to as the 'reference section length'. Moreover, reference locations and the corresponding lag distances depend on the speed profile assigned.

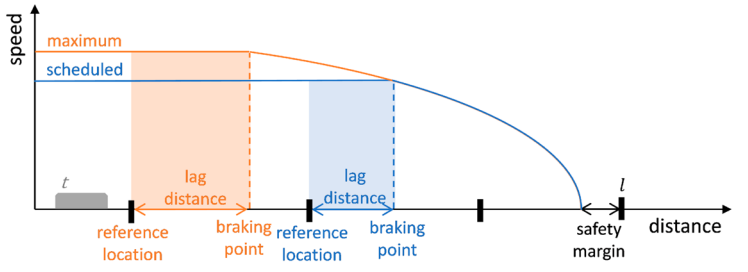

(a) For maximum and scheduled speed profiles.

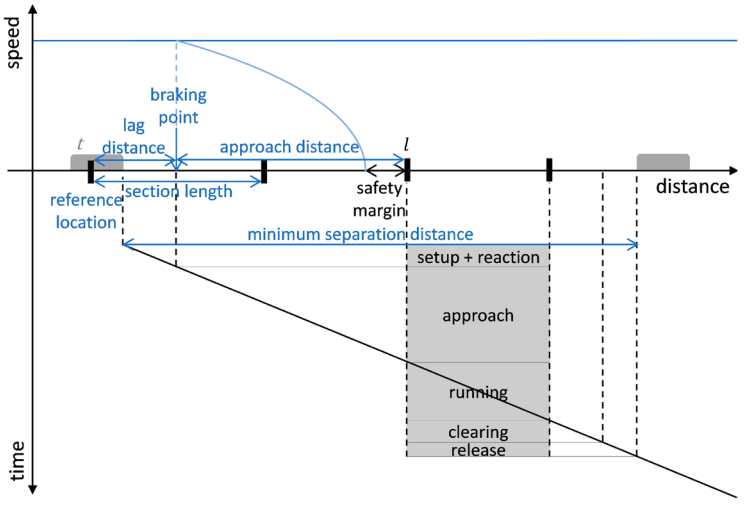

(b) Train blocking time components related to minimum train separation for scheduled speed profile.

Figure 4. Modelling concept including braking points, reference (brake) locations and (reservation) lag distances for train *t* approaching location *l*. (a) For maximum and scheduled speed profiles and (b) Train blocking time components related to minimum train separation for scheduled speed profile.

In addition to the definition of the reference brake location, we enable the modelling of continuous braking curve supervision. Indeed, the blocking of a location by an approaching train starts at the moment the train passes the braking point, minus the setup and reaction time, rather than the associated reference brake location. This implies that only if a train's MA reaches beyond a certain location, it can pass the braking point associated with that location. For the approximation of the passing times at braking points, we introduce the concept of *reservation lag*. For a specific speed profile, the reservation lag indicates the time interval by which the reservation can be postponed, with respect to the passing time of the corresponding reference location. Hence, it is the time it takes the train to traverse the above defined lag distance, which is approximated by the following formula:

$$\text{reservation lag} = \frac{\text{lag distance}}{\text{reference section length}} \text{ running time over reference section,}$$

with the reservation lag and running time in seconds and the lag distance and section length in metres. Note that the values of all terms but the reference section length depend on the speed profile.

The modelling concept for fixed-block DTG signalling is illustrated in Figure 4. Figure 4(a) indicates the speed-dependent reference (brake) locations and associated lag distances for train *t* approaching location *l* according to its maximum or scheduled profile, respectively. It shows that the *maximum-speed reference location* lies before the *scheduled-speed reference location* since the higher the speed, the longer the braking distance. It also shows that the lag distances, or the reservation lags, for the maximum and scheduled speed profiles are not equal as they depend on the braking point in relation to the discretisation grid. In Figure 4(b), the reference location and lag distance for the scheduled speed profile are related to the approach distance and the reference section length. Also, the blocking time components are related to the train separation. We note that the trains in the figure are separated by the minimum separation distance under worst-case conditions, i.e. the largest value that the minimum separation can take.

We note that this enhancement does not modify the blocking time theory but only allows to provide a more accurate computation of train blocking times to capture the signalling feature of braking curve supervision.

4. Enhancement of RECIFE-MILP to distance-to-go signalling

In this section, we apply the proposed enhancements to the state-of-the-art fixed-block RECIFE-MILP model (Pellegrini et al. 2015), obtaining a MILP formulation of a CDR model for DTG signalling. First, we shortly describe the RECIFE-MILP model from the literature (Section 4.1). Second, we provide the mathematical formulation resulting from enhancing RECIFE-MILP (Section 4.2).

4.1. The RECIFE-MILP model

RECIFE-MILP is a CDR model for conventional fixed-block signalling developed by Pellegrini, Marlière, and Rodriguez (2014) and Pellegrini et al. (2015). The model features a microscopic representation of the infrastructure, in terms of TDSs grouped into blocks. A train route is considered as a sequence of TDSs from its entry to its exit of the considered infrastructure.

Due to the implementation of the route-locking sectional-release principle, the blocking time of a TDS for a train includes the setup and reaction time (together: the formation time), the time to run with the train's head from the entry of the reference block a fixed number of blocks in advance to the entry of the TDS (the approach time), the time to run with the train's head from the entry to the exit of the TDS (the running time), the time to run with the train's length over the TDS exit (the clearing time), and the release time (Hansen and Pachl 2014).

RECIFE-MILP is a fixed-speed model assuming minimum train running and clearing times, and dismissing speed dynamics in case of unplanned declarations or stops. Station dwell times and delays are included in the model as extended occupation times. The objective of RECIFE-MILP is to minimise the weighted cumulative total delay, i.e. the delays of all trains upon entering the infrastructure, upon arriving at scheduled stops and upon exiting the considered infrastructure (or upon reaching its final destination). To this end, the model allows for retiming, reordering and rerouting of trains.

RECIFE-MILP has been applied to various case studies and has been proven to perform well in real-time applications (Pellegrini et al. 2015). Also, the model has been evaluated in open- and closed-loop frameworks with a simulation environment (Pellegrini, Marlière, and Rodriguez 2016; Quaglietta et al. 2016), enabling a realistic assessment of the implications of the rescheduling decisions optimised under the fixed-speed assumption. For the mathematical formulation of RECIFE-MILP and further details, we refer to Pellegrini, Marlière, and Rodriguez (2014), Pellegrini et al. (2015) and Pellegrini, Pesenti, and Rodriguez (2019).

4.2. MILP formulation for distance-to-go conflict detection and resolution

Here, we present the new mathematical model of RECIFE-MILP for DTG signalling. The sets, parameters and variables, as well as the objective function and the constraints of the MILP formulation for DTG CDR are included. Note that not all details of the RECIFE-MILP model are given here. For that, we refer the reader to Pellegrini, Marlière, and Rodriguez (2014), Pellegrini et al. (2015) and Pellegrini, Pesenti, and Rodriguez (2019).

4.2.1. Sets, parameters and variables

In this section, we describe the sets, parameters and variables of the model, as listed in Table A1. In both Table A1 and the following descriptions, newly introduced and updated modelling elements are indicated in **bold**.

The sets represent collections of elements that are used for the model notation. The four main sets are the set of trains T, the set of routes R, the set of locations L and the set of stations S. Subsets $R_t \subset R$ and $S_t \subset S$ are defined to represent routes and stations relevant to train $t \in T$.

For the set of locations, multiple subsets are defined. First, the subsets indicating the relevant locations per train $L_t \subset L,\ t \in T$ and per route $L^r \subset L,\ r \in R$. Next, the sets of *occupied locations* $OL_{t,r,l} \subset L^r$, containing the locations along route $r \in R_t$ for which it holds that if train $t \in T$ starts occupying it, the train has not yet cleared location $l \in L^r$. $L_{t,s} \subset L_t$ is the set of locations that can be used by train $t \in T$ to stop at station $s \in S_t$. $\hat{L}_{t,t',l} \subset L_t \cap L_{t'}$ is the set of locations that trains $t,\ t' \in T$ need to traverse in the same order, i.e. if train t precedes t' on $l \in L$, then t precedes t' on $l' \in \hat{L}_{t,t',l}$. Finally, the set of speed assignment locations $\mathbf{P} \subset \boldsymbol{L}$ containing the track locations to which a speed profile is assigned for the whole track. Subset $\mathbf{P^r} \subset \mathbf{P}$ contains the speed assignment locations along route $r \in R$.

The parameters are provided as input to the model. First, parameters related to the infrastructure. $\pi_{r,l}$ and $\sigma_{r,l}$ are defined to represent the preceding and succeeding location of location $l \in L^r$ along route $r \in R$, respectively. $\boldsymbol{\rho_{r,l} \in \mathbf{P^r}}$ indicates the speed assignment location associated with location $l \in L^r$ along route $r \in R$. As mentioned in Section 3.2, it is the first location of the track to which l belongs. Additionally, $\boldsymbol{s_l}$ indicates whether location $l \in L$ is a switch location ($s_l = 1$), or a track location ($s_l = 0$). Also, dummy location $l_\infty \in L$ represents the dummy destination of all trains, added at the end of each route.

Next, we define the parameters related to the timetable. The initial entry time and the scheduled destination arrival time of train $t \in T$ are given by $init_t$ and $sched_t$, respectively. The minimum dwell time of train $t \in T$ at station $s \in S_t$ is given by $dw_{t,s}$. The

arrival and departure time of train $t \in T$ at station $s \in S_t$ are given by $a_{t,s}$ and $d_{t,s}$, respectively.

Then, we define the parameters related to the blocking times. The formation time, which includes the setup and reaction time, and the release time of location $l \in L^r$ along route $r \in R$ are given by $for_{r,l}$ and $rel_{r,l}$, respectively. The running time of train $t \in T$ from location $l \in L_t$ to its succeeding location $\sigma_{r,l} \in L^r$ along route $r \in R_t$ is described by two parameters. $rt_{t,r,l}$ gives the minimum running time corresponding to running according to the maximum speed profile. $\boldsymbol{\Delta rt_{t,r,l}}$ gives the additional running time in case the train follows a scheduled speed profile. Similarly, the clearing time of train $t \in T$ of location $l \in L^r$ along route $r \in R_t$ is given by the minimum clearing time $cl_{t,r,l}$ and the possible additional clearing time $\boldsymbol{\Delta ct_{t,r,l}}$.

A second group of parameters is related to the approach time: the reference (brake) locations and the reservation lags. They are defined in line with their introduction in Section 3.3. Locations $\boldsymbol{ref^{s}_{t,r,l}}$, $\boldsymbol{ref^{m}_{t,r,l}} \boldsymbol{\in L^r}$ represent the reference brake locations for location $l \in L^r$ along route $r \in R_t$ for train $t \in T$ approaching according to the scheduled or maximum speed profile, respectively. Reservation lag parameters $\boldsymbol{lag^{s}_{t,r,l}}$ and $\boldsymbol{lag^{m}_{t,r,l}}$ are defined to indicate the time by which the reservation of location $l \in L^r$ along route $r \in R_t$ for train $t \in T$ can be postponed after passing the corresponding reference brake location. We refer back to Figure 4 for the illustration of the reference brake location and reservation lags.

Finally, we define M to be a large constant and the weights w and w_t, $t \in T$, for the objective function. $\boldsymbol{w}$ is a penalty weight for the assignment of maximum speed profiles and w_t is a priority weight for train t and its delay.

The model variables are either binary decision variables or continuous timing variables. The binary decision variables capture the scheduling and speed profile decisions. The passing order of two trains $t, t' \in T$ at common location $l \in L_t \cap L_{t'}$ is determined by variable $y_{t,t',l}$. The order variables are only defined for one representative location per $\hat{L}_{t,t',l}$ set. Recall that within $\hat{L}_{t,t',l}$, train orders do not change. The route assignment of train $t \in T$ is captured by variable $x_{t,r}$, indicating for route $r \in R_t$ whether or not the route is used by train t. The assignment of speed profiles is described by two different sets of variables. $\boldsymbol{v^{s}_{t,r,l}}$ indicates whether or not train $t \in T$ runs according to the scheduled speed profile over speed assignment location $l \in \mathrm{P}^r$ along route $r \in R_t$, while $\boldsymbol{v^{m}_{t,r,l}}$ indicates whether or not train $t \in T$ runs according to the maximum speed profile over speed assignment location $l \in \mathrm{P}^r$ along route $r \in R_t$.

The timing variables include the decision variables that indicate the physical occupation starting time: $o_{t,r,l}$ with $t \in T$, $r \in R_t$ and $l \in L^r$. Additionally, we have timing variables that depend on the occupation starting time and the binary decision variables. These auxiliary variables represent the extended physical occupation times due to dwell time, delay and/or scheduling decisions ($o^{+}_{t,r,l}$ with $t \in T$, $r \in R_t$ and $l \in L^r$), the blocking starting and ending times ($b^{s}_{t,l}$ and $b^{e}_{t,l}$ with $t \in T$ and $l \in L_t$), the final delays (z_t with $t \in T$), and the delays at scheduled stops ($z_{t,s}$ with $t \in T$ and $s \in S_t$).

4.2.2. Objective function

In line with the general objective of rescheduling in case of disturbances (Cacchiani et al. 2014), the main objective of the model is to minimise total train delay. As secondary objective, we want to enforce the assignment of scheduled speed profiles where possible.

This results in the following objective function:

$$\text{minimise} \sum_{t \in T} \left(w_t \left(z_t + \sum_{s \in S_t} z_{t,s} \right) + w \sum_{\substack{r \in R_t: \\ l \in \mathrm{P}^r}} v^{\mathrm{m}}_{t,r,l} \right). \tag{2}$$

The first term includes the weighted cumulative delay, i.e. the weighted sum of train delays upon arriving at scheduled stops ($z_{t,s}$ with $t \in T$ and $s \in S_t$) or upon exiting the infrastructure, either by leaving the area or by reaching its terminus (z_t with $t \in T$). The weights w_t, $t \in T$ can, for example, be interpreted as priority factors.

The second term counts the number of maximum speed profiles assigned. With maximum speed profiles only assigned when it reduces total delay by more than w seconds, it can be ensured that typically more energy-efficient scheduled speed profiles are assigned by default. To align with the secondary nature of this objective, weight w should be at most 1. From here on, this second term is also referred to as *speed penalty*.

4.2.3. Constraints

The constraints describing the DTG version of RECIFE-MILP are given by Equations (3) to (18). Compared to the original MILP, Constraints (6), (13), (14) and (15) are new, Constraints (7), (10), (12) and (16) are changed, and Constraints (3), (4), (5), (8), (9), (11), (17) and (18) are the same. The presented constraints are explained in the following. For the changed constraints, we add a short description of how they differ from the original version.

$$o_{t,r,l} \geq init_t \, x_{t,r} \quad \forall t \in T,\ r \in R_t,\ l \in L^r, \tag{3}$$

$$o_{t,r,l} \leq M \, x_{t,r} \quad \forall t \in T,\ r \in R_t,\ l \in L^r, \tag{4}$$

$$\sum_{r \in R_t} x_{t,r} = 1 \quad \forall t \in T, \tag{5}$$

$$v^{\mathrm{m}}_{t,r,l} + v^{\mathrm{s}}_{t,r,l} = x_{t,r} \quad \forall t \in T,\ r \in R_t,\ l \in \mathrm{P}^r, \tag{6}$$

$$o_{t,r,\sigma_{r,l}} = o_{t,r,l} + o^{+}_{t,r,l} + rt_{t,r,l} \, x_{t,r} + \Delta rt_{t,r,l} v^{\mathrm{s}}_{t,r,\rho_{r,l}} \quad \forall t \in T,\ r \in R_t,\ l \in L^r, \tag{7}$$

$$o^{+}_{t,r,l} \geq \sum_{\substack{s \in S_t: \\ l \in S_{t,s} \cap L^r}} dw_{t,s} \, x_{t,r} \quad \forall t \in T,\ r \in R_t,\ l \in \bigcup_{s \in S_t} L_{t,s}, \tag{8}$$

$$o_{t,r,\sigma_{r,l}} \geq \sum_{\substack{s \in S_t: \\ l \in L_{t,s} \cap L^r}} d_{t,s} \, x_{t,r} \quad \forall t \in T,\ r \in R_t,\ l \in \bigcup_{s \in S_t} L_{t,s}, \tag{9}$$

$$z_{t,s} \geq \sum_{r \in R_t} \sum_{l \in L^r \cap L_{t,s}} \left(o_{t,r,l} + rt_{r,t,l} x_{t,r} + \Delta rt_{t,r,l} v^{\mathrm{s}}_{t,r,\rho_{r,l}} \right) - a_{t,s} \quad \forall t \in T, s \in S_t, \tag{10}$$

$$z_t \geq \sum_{r \in R_t} o_{t,r,l_\infty} - sched_t \quad \forall t \in T, \tag{11}$$

$$b^{\mathrm{s}}_{t,l} \leq \sum_{\substack{r \in R_t: \\ l \in L^r}} \left(o_{t,r,ref^{\mathrm{s}}_{t,r,l}} + \left(lag^{\mathrm{s}}_{t,r,l} - for_{r,l} \right) x_{t,r} \right) \quad \forall t \in T,\ l \in L_t : s_l = 0 \vee \nexists r \in R_t : s_{\pi_{r,l}} = 1, \tag{12}$$

$$b^{\mathrm{s}}_{t,l} \leq \sum_{\substack{r \in R_t: \\ l \in L^r}} \left(o_{t,r,ref^{\mathrm{m}}_{t,r,l}} + \left(lag^{\mathrm{m}}_{t,r,l} - for_{r,l} \right) x_{t,r} + M\, v^{\mathrm{s}}_{t,r,\rho_{r,ref^{\mathrm{s}}_{t,r,l}}} \right)$$

$$\forall t \in T,\ l \in L_t : s_l = 0 \vee \nexists r \in R_t : s_{\pi_{r,l}} = 1, \tag{13}$$

$$b^{\mathrm{s}}_{t,l} \leq \sum_{\substack{r \in R_t: \\ l \in L^r}} (o_{t,r,ref^{\mathrm{s}}_{t,r,\pi_{r,l}}} + \left(lag^{\mathrm{s}}_{t,r,\pi_{r,l}} - for_{r,\pi_{r,l}} \right) x_{t,r}$$

$$\forall t \in T,\ l \in L_t : s_l = 1 \wedge \exists r \in R_t : s_{\pi_{r,l}} = 1, \tag{14}$$

$$b^{\mathrm{s}}_{t,l} \leq \sum_{\substack{r \in R_t: \\ l \in L^r}} \left(o_{t,r,ref^{\mathrm{m}}_{t,r,\pi_{r,l}}} + \left(lag^{\mathrm{m}}_{t,r,\pi_{r,l}} - for_{r,\pi_{r,l}} \right) x_{t,r} + M\, v^{\mathrm{s}}_{t,r,\rho_{r,ref^{\mathrm{s}}_{t,r,\pi_{r,l}}}} \right)$$

$$\forall t \in T,\ l \in L_t : s_l = 1 \wedge \exists r \in R_t : s_{\pi_{r,l}} = 1, \tag{15}$$

$$b^{\mathrm{e}}_{t,l} = \sum_{\substack{r \in R_t: \\ l \in L^r}} \left(o_{t,r,\sigma_{r,l}} + \left(ct_{t,r,l} + rel_{r,l} \right) x_{t,r} + \Delta ct_{t,r,l} v^{\mathrm{s}}_{t,r,\rho_{r,l}} + \sum_{\substack{l' \in L^r: \\ l' \in OL_{t,r,l}}} o^{+}_{t,r,l'} \right)$$

$$\forall t \in T,\ l \in L_t, \tag{16}$$

$$b^{\mathrm{e}}_{t,l} - M\,(1 - y_{t,t',\hat{\jmath}}) \leq b^{\mathrm{s}}_{t',l} \quad \forall t, t' \in T, \text{index } t < \text{index } t',\ l, \hat{l} \in L_t \cap L_{t'} : l \in \hat{L}_{t,t',\hat{\jmath}}, \tag{17}$$

$$b^{\mathrm{e}}_{t',l} - M\, y_{t,t',\hat{\jmath}} \leq b^{\mathrm{s}}_{t,l} \quad \forall t, t' \in T, \text{index } t < \text{index } t',\ l, \hat{l} \in L_t \cap L_{t'} : l \in \hat{L}_{t,t',\hat{\jmath}}. \tag{18}$$

Constraints (3) force train t to start operating no earlier than its initial entry time $init_t$ on its assigned route, while Constraints (4) set the occupation starting time of all locations along the train's unassigned routes to zero. Constraints (5) ensure that a single route is assigned to each train.

Constraints (6) ensure that either a maximum or a scheduled speed profile is assigned to speed assignment locations along the route of a train. No speed profile is assigned to locations along routes that are not assigned to the train ($v^{\mathrm{m}}_{t,r,l} = v^{s}_{t,r,l} = 0$).

Constraints (7) describe the difference in occupation starting times between succeeding locations in terms of extended occupation time and running time. By Constraints (8), the extended occupation time $o^{+}_{t,r,l}$ includes the dwell time at scheduled stops. Additionally, it includes the difference in running time in case the assigned speed profile cannot be followed due to a delayed train in front. The running time of a train from a location to the succeeding one depends on the assigned speed profile. If train t runs over location l along route r according to the maximum speed profile, i.e. $v^{\mathrm{m}}_{t,r,\rho_{r,l}} = 1$ and hence $v^{\mathrm{s}}_{t,r,\rho_{r,l}} = 0$, then only the minimum running time $rt_{t,r,l}$ is considered. If train t runs over location l along route r according to the scheduled speed profile, i.e. $v^{\mathrm{s}}_{t,r,\rho_{r,l}} = 1$, then the additional running time $\Delta rt_{t,r,l}$ is also included. This additional running time term is the DTG addition to the original constraints.

Constraints (8) ensure that the station dwell times are included in the extended occupation time, while Constraints (9) ensure that train t does not leave its stopping location $l \in L_{t,s}$ before its scheduled departure time from station s.

Constraints (10) and (11) quantify non-negative delay at each station where train t has a scheduled stop ($z_{t,s}$) and at its exit from the infrastructure and/or when reaching its final destination (z_t). Note that t is assumed to stop at the end of the TDS where the stop occurs. In Constraints (10), the occupation starting time of train t on the stopping location along route r at station s is compared with its scheduled arrival time at station s ($a_{t,s}$). For DTG, the speed-dependency of the running time over the stopping TDS is included. In Constraints (11), the occupation starting time of train t on the dummy destination location is compared with the scheduled exit time ($sched_t$).

Constraints (12) to (15) set the blocking starting times. Constraints (12) and (13) describe the speed-dependent blocking starting times of track locations, i.e. location l such that $s_l = 0$, and of locations that can be the first of a switch area for a specific train, i.e. location l such that $\nexists r \in R_t : s_{\pi_{r,l}} = 1$.

Constraints (12) ensure that the blocking of track location l by train t starts at the latest the formation time before the train passes the braking point corresponding to the scheduled speed profile, that is the moment the train starts occupying the scheduled-speed reference location $ref^{\mathrm{s}}_{t,r,l}$ along the assigned route, postponed with the scheduled-speed reservation lag $lag^{\mathrm{s}}_{t,r,l}$. Indeed, the blocking of a track location starts earlier when a train is approaching according to the maximum speed profile than to the scheduled speed profile because of the longer braking curve (see Figure 4(b)).

This constraint differs from the fixed-block version in two main ways. First, it has become an inequality rather than an equality constraint due to the introduction of a speed profile alternative. Second, the right term is redefined to correspond to the braking point which can lie anywhere on the track rather than the entry of the train- and speed-independent reference block in the fixed-block model.

Constraints (13) ensure that in case the approaching train is running according to the maximum speed profile, the blocking starts earlier. Namely, at the moment the train passes the maximum-speed braking point ($o_{t,r,ref^{\mathrm{m}}_{t,r,l}} + lag^{\mathrm{m}}_{t,r,l}$) along the assigned route, minus the formation time. However, the blocking starting time in case of a train approaching according to the scheduled speed profile must not be restricted. For that purpose, a big-M term is added. The value of M should include the running time from the maximum-speed braking point to the scheduled-speed brake starting point and the possible longer stay at the locations in between.

Constraints (14) and (15) deal with the locations in switch areas that are not the first switch location for a specific train, i.e. with $l : s_l = 1$ while $\exists r \in R_t : s_{\pi_{r,l}} = 1$. The blocking of such a switch location starts as soon as the preceding location would start being blocked (if not also the exit of a switch section). Hence, Constraints (14) and (15) are the same as Constraints (12) and (13), except that they refer to (the braking point of) the preceding location.

Constraints (16) set the blocking ending times. The blocking of a location lasts until the train has fully passed the succeeding location along its route, plus the release time. The clearing time is included in the blocking time. In case of a maximum speed profile, only the minimum clearing time is considered, while in case of a scheduled speed profile, an additional clearing time component is included. This speed-dependent term in the clearing time is the DTG alteration to the original constraint. Additionally, if the train is long enough to keep occupying a location when its head is at the following locations (included in set $OL_{t,r,l}$), also the extended occupation times of the train for these locations has to be accounted for.

Finally, disjunctive Constraints (17) and (18) ensure that the location blocking times of two trains do not overlap, depending on train orderings. The passing order of a pair of trains is defined per set of locations that the two trains need to pass in the same order.

5. Results

In this section, we present the results of the assessment of the fixed-block DTG CDR model obtained by enhancing RECIFE-MILP. The assessment is carried out through model experiments in two distinct case studies, which are introduced in Section 5.1. To evaluate the applicability to DTG and the operational performance of the model, we conduct a comparative analysis between the enhanced model and the original model for conventional fixed-block signalling. The model solutions are compared in terms of the objective function, the underlying rescheduling decisions and the effects of the model enhancements, specifically the shorter train separation due to the introduction of train- and speed-dependent blocking times and brake indication points. The results of the comparative analysis under the setup presented in Section 5.2 are discussed in Section 5.3. To further illustrate the model for fixed-block DTG operations, we zoom in on a specific case study instance in Section 5.4.

We run the experiments on an Intel(R) Xeon(R) CPU Gold 6226R CPU @ 2.90GHz, 16 cores, 256 GB RAM. The implementation uses IBM ILOG CPLEX Concert Technology for C++, version 20.1. The optimisation models are run to find the rescheduling decisions that give the minimum objective value. The computation time limit is set to 3600 seconds to seek optimality; we obtain a maximum optimality gap of 0.68%. With this, the time limit does not correspond to a real-time application, but it allows for a thorough assessment of the enhanced model: we aim to understand whether the model enhancements indeed result in a better description of ETCS L2 operations and, if so, whether they lead to different rescheduling decisions to be optimal. Given the foreseen real-time implementation, a discussion of the real-time applicability of the model is added in Section 5.5.

5.1. Case studies

The model experiments are performed in two case studies representing traffic control areas in France: the Gonesse junction and the Rosny-StEtienne corridor. The Gonesse area is a 17-kilometre long complex junction with dense mixed traffic. Figure 5(a) provides a schematic representation of the Gonesse junction. The junction includes 89 TDSs with lengths ranging from 35 to 2424 metres, with a mean of 560 metres. The TDSs are grouped into 79 blocks and 37 routes. It has no platforms. The timetable of a weekday includes 336 trains, of which 116 high-speed, 129 conventional, and 91 freight trains, with 5 to 13 route alternatives per train.

The Rosny-StEtienne area is a 68-kilometre long corridor of the Paris-Le Havre line with mixed traffic. Figure 5(b) provides a schematic representation of the Rosny-StEtienne corridor. The corridor includes 239 TDSs with lengths ranging from 100 to 2217 metres, with a mean of 740 metres. The TDSs are divided over 152 blocks and 169 routes. It has 10 stations with a total of 39 platform tracks. Its daily timetable features 215 trains, of which 2 high-speed, 122 conventional, 56 freight and 35 empty (including work and test) trains, with 1 to

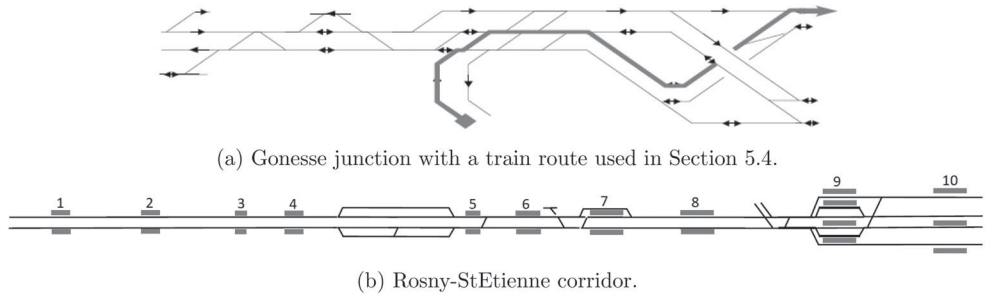

(a) Gonesse junction with a train route used in Section 5.4.

(b) Rosny-StEtienne corridor.

Figure 5. Schematic track layouts of the traffic control areas consider in the case studies. (a) Gonesse junction with a train route used in Section 5.4 and (b) Rosny-StEtienne corridor.

24 route alternatives each. We note that the Rosny-StEtienne corridor is not a high-speed line, so high-speed trains use the maximum speed of conventional trains.

The two areas are equipped with conventional fixed-block signalling systems featuring more than three aspects. We note that the Gonesse junction features signals with different numbers of aspects, and that the blocks in the Rosny-StEtienne corridor are shorter than in the Gonesse area.

For both traffic control areas, 100 delay scenarios are generated based on a one-day timetable, where entry delays between 5 and 15 minutes are imposed on 20% of the trains. Both the selection of the affected trains and the magnitude of their entry delays are determined randomly, using uniform probability distributions. This introduces stochasticity into the scenario generation process and ensures an unbiased variety of delay scenarios, consistent with the approaches of Lusby et al. (2013) and Pellegrini, Marlière, and Rodriguez (2014). These delay scenarios are considered in a one-hour period, i.e. the peak hour from 18:00 to 19:00. For the selection of trains entering and/or starting in the traffic control area within the hour, retiming, reordering and rerouting options are taken into consideration.

The case studies are applied in the two versions of the RECIFE-MILP model: in a DTG/ETCS L2 variant of the enhanced model as well as in the original model for conventional fixed-block signalling. As (only) conventional fixed-block signalling is implemented in the considered areas, we project the DTG principles of ETCS L2 on the case studies. While the same MILP formulation is applied to the two case studies for each of the model versions, the differing characteristics, such as track layout and traffic pattern, lead to distinct models in terms of, e.g. size and outcome. For the two model versions, Table 2 presents insights on the model size, including the number of binary variables, continuous variables and constraints for both the junction and the corridor area. Based on the presented numbers, two points are worth noting.

First, the ETCS L2 model is larger than the original. The addition of speed profile options into the model leads to a significant increase in binary variables and a slight increase in constraints. The number of continuous variables stay the same as the number of timing variables are independent of speed modelling.

Second, the two case studies differ substantially in terms of the number of the three model components. Compared to the corridor case study, the junction case study features

Table 2. Number (#) of binary and continuous variables, and constraints in ETCS L2 and original, i.e. conventional fixed-block, model versions.

	ETCS L2	Original
Junction		
# binary variables	6186	3784
# continuous variables	28844	28844
# constraints	81407	78476
Corridor		
# binary variables	4649	665
# continuous variables	68902	68902
# constraints	113214	109887

more binary variables, but significantly less continuous variables and also slightly less constraints. The latter two are in line with the 89 versus 239 TDSs. The binary variables are the route, order and speed variables. Route variables are balanced out with more routes, but less trains. With the difference in number of binary variables being the most substantial in the original model, it is not so much related to the speed variables, but rather to the order variables. In areas similar to the considered corridor area, the number of order variables can be seriously reduced due to the definition of $\hat{L}_{t,t',l}$, i.e. the set of locations which may be used by trains $t, t' \in T$ such that if t precedes t' on l, then t precedes t' on l'.

5.2. Model parameter setup

For model initialisation, we rely on input data available for the original fixed-block version of RECIFE-MILP. We make the following assumptions related to the three enhancements.

First, the assumptions concerning the track. For ETCS L2, we consider a discretisation of the track based on TDSs, refraining from the conventional fixed blocks. In line with that, reservation and release of the track is modelled at TDS level, and locations refer to the entries of the TDSs. The entry point of a TDS containing a switch, is a switch location. Otherwise, it is a track location.

Switch locations lie in the same switch area if they are not separated by a track location. Hence, a switch area consists of a collection of consecutive switch locations, and two switch areas are separated by at least one block/TDS, which can be assumed to be longer than a (passenger) train length with typical lengths of well over 200 metres.

Second, the assumptions related to the speed profile options. The maximum speed of a train at a location is the minimum between the maximum track speed at the location and the maximum train speed. The scheduled speed equals the maximum speed in switch areas, and is assumed to be 80% of the maximum speed on the track. Correspondingly, the additional running and clearing times of the scheduled speed profile with respect to the maximum one are 0% in switch areas and at most 25% on the track. We note that this assumption leads to a discontinuity in train speed profiles at the borders of switch areas, which we consider a consequence of the model being a fixed-speed model.

All weight factors in the objective function are set to be 1. With $w_t = 1$ for all trains $t \in T$, no trains are prioritised over other trains. With $w = 1$, it is counted how often a maximum speed profile is assigned. A positive weight ensures that a maximum speed profile is only assigned if it results in some delay recovery. If the weight is higher, the assignment of maximum speed profiles is actively penalised. Then, minimum running times will be less often

considered. A higher weight would give the ETCS L2 model a disadvantage compared to the conventional fixed-block model and hence, result in an unfair assessment.

Third, the assumptions related to the DTG blocking times. The formation and release times of a location equal the ones of the block they belong to in the conventional fixed-block model. These values are mostly based on the presence of trackside train detection, which is still the case in ETCS L2. For the computation of the brake locations (Equation (1)), we assume the train braking rates to be constant and the deceleration due to resistance to be negligible. The safety margin is 50 metres (PERFORMINGRAIL 2022). We note that these assumptions are made for ease of computation. In practice, they can easily be changed with more accurate values.

Recall that in the original fixed-block model, we use the minimum running and clearing times computed considering maximum speed profiles. By doing so, we are being conservative. If a bias on delay assessment is introduced, it will be in favour of the original fixed-block model rather than of the enhanced DTG model that we aim to verify.

5.3. Comparative analysis

We present the results of the comparative analysis in two steps. First, we focus on the comparison of the ETCS L2 with the conventional fixed-block results in terms of the model objective components. Second, we discuss the underlying rescheduling solutions in more detail. In both steps, we consider the optimisation of the ETCS L2 and the original model for conventional fixed-block signalling as well as their cross-evaluations 'ETCS L2 in original' and 'original in ETCS L2'. By evaluating optimised solutions from one model version, e.g. the original model, in the other model version, e.g. the enhanced model, we analyse how the rescheduling decisions obtained in the context of one signalling system, e.g. conventional fixed block, affect the train delays when implemented under different signalling constraints, e.g. ETCS L2.

The optimisation results of the ETCS L2 and original model in terms of the model objective components are given in the first and last column of Table 3, respectively. These are the mean total delay and the mean delay recovery over all scenarios. Note that speed penalties are only included in the objective of the ETCS L2 model. The mean total delays obtained by the ETCS L2 optimisation are 7015 and 5530 seconds for the junction and corridor, respectively. The corresponding delay recovery percentages are 10.89% and 55.33%. With the original optimisation, mean total delays of 7325 and 5576 seconds are obtained for the respective case studies, with corresponding delay recovery percentage of 8.57% and 50.73%. Comparing the results, we see that the ETCS L2 model significantly improves upon the original model regarding delay. The respective improvements for the two case studies are 4.23% and 0.82% in terms of total delay and 27.07% and 5.13% in terms of delay recovery.

Table 3 also reports the results of the cross-evaluations of the model solutions. First, the evaluation of the ETCS L2 solution in the original model: the scheduling decisions made in the ETCS L2 solutions are applied considering conventional fixed-block signalling. This evaluation is an additional check on the distinctness of the optimised rescheduling decisions of the models. If the ETCS L2 rescheduling decisions lead to the same objective value as the rescheduling decisions in the original model, then the ETCS L2 solution is an alternative optimal conventional fixed-block solution. Similarly, the evaluation of the original

Table 3. Mean total delay, delay recovery and number of maximum speed profile assignments (speed penalty) of optimisation and cross-evaluation of ETCS L2 and original, i.e. conventional fixed-block, model.

	ETCS L2	Original in ETCS L2	ETCS L2 in original	Original
Junction				
Total delay (s)	7015	7062	7599	7325
Delay recovery (%)	10.89	10.39	6.96	8.5
Speed penalty (–)	46	58	–	–
Corridor				
Total delay (s)	5530	5520	5590	5576
Delay recovery (%)	53.33	53.58	53.13	50.73
Speed penalty (–)	10	29	–	–

rescheduling decisions in the ETCS L2 model can indicate that the original solution is an alternative optimal solution for the ETCS L2 model. In the case of either of the two situations, we dismiss the solution differences in the further analysis of the scenario.

From the evaluation of the ETCS L2 solution in the original model, it is clear that the ETCS L2 and original solutions contain different rescheduling decisions. With mean total delays of 7599 and 5590 s for the different case studies, the ETCS L2 solution performs 8.33% worse in the junction and 1.08% worse in the corridor when applied in fixed block. These differences originate from the different minimum train separation distances. Compared to the original optimisation, the ETCS L2 in original total delays are 3.74% worse in the junction but only 0.25% worse in the corridor. This underlines the occurrence of different optimal rescheduling solutions due to these distinct minimum train separations.

The evaluation of the original solution in the ETCS L2 model provides insight into the extent to which the improvement of ETCS L2 over conventional fixed-block originates from the ETCS L2 blocking times or from the possibly different rescheduling decisions in the respective solutions. The mean total delays of the cross-evaluation of conventional fixed-block in ETCS L2 are 7062 s for the junction case study and 5520 s for the corridor case study. With this, evaluating the original solution in the ETCS L2 model already improves the total delay with 3.59% and 1.00% for the junction and corridor case studies, respectively. So, most of the ETCS L2 over conventional fixed-block improvement originates from the ETCS L2 blocking times. Notwithstanding the slight improvement of the ETCS L2 solution over the original solution that is due to the different rescheduling decisions (ETCS L2 over original in ETCS L2): from 3.59% to 3.74% for the junction and 1.00% to 1.72% for the corridor. We also note the difference in speed penalty between ETCS L2 and original in ETCS L2. In the ETCS L2 solutions, trains run less often according to maximum speed profiles. Therefore, these solutions will also be beneficial in terms of energy consumption.

To better understand the role of the rescheduling solutions, we take a closer look at the case study instances. Specifically, we are interested in the instances for which the ETCS L2 model finds rescheduling decisions that are different from those in the (conventional) fixed-block solution and that outperform the latter in terms of objective value. As these instances benefit from the ETCS L2 optimisation, they are referred to as 'improved instances'. The percentage of improved instances per case study is reported in Table 4, together with the number of different ordering and routing decisions of ETCS L2 relative to conventional fixed block. In the junction case study, 98% of the instances are improved by ETCS L2 relative to conventional fixed block. For the corridor case study, this is the case for 55%.

Table 4. Case study results for ETCS L2 relative to conventional fixed block.

Case study	% improved instances	# Δ ordering decisions		# Δ routing decisions	
Junction	98	max	4	max	13
		mean	0.31	mean	7.40
Corridor	55	max	2	max	11
		mean	0.11	mean	2.87

Considering all 100 instances for the junction case study, the number of different ordering and routing decisions ranges from 0 to 4 with a mean of 0.31, and from 0 to 13 with a mean of 7.40, respectively. Over the 100 instances in the corridor case study, the number of different ordering and routing decisions range from 0 to 2 with a mean of 0.11 and from 0 to 11 with a mean of 2.87, respectively. So, the mean numbers of different routing decisions are a factor of 24 and 26 higher than the mean numbers of different ordering decisions in the junction and corridor case studies, respectively. On its own, one different rerouting typically offers a minimum improvement. However, some routes seem to be preferable for some trains. Moreover, different routes are becoming attractive due to the short blocking times in general.

Overall, the results of the ETCS L2 model are not striking when comparing the rescheduling solutions (in the ETCS L2 model) with mean relative reductions in objective values of 0.85% and 0.17%. However, for specific instances, the model can have a remarkable impact: up to 7.09% reduction in objective value. For all instances, the ETCS L2 optimisation proposes solutions that are at least as good as the conventional fixed-block solution when evaluated in the ETCS L2 model.

From the results, we conclude that (the modelling of) DTG has more impact on CDR in the junction than in the corridor. The percentage of instances improved by ETCS L2 and the relative reduction in objective value is higher. An important factor in this is the traffic density, which is about a factor 1.5 higher in the junction than in the corridor: 336 versus 215 trains on a daily basis and 29 versus 19 trains in the considered hour. Moreover, the difference in track layout affects the attractiveness of alternative routes. The number of alternative routes is higher in the corridor, while the number of different routing decisions is higher in the junction. The corridor features double-track lines for traffic running in two directions, encouraging the separation of the two flows. The junction features overlapping lines in various directions, making flow separation practically impossible.

5.4. Detailed analysis of an improved instance

In this section, we further illustrate the model for DTG operations by zooming in on a specific case study instance. We aim to analyse in detail the 'what and why', e.g. related to the DTG modelling principles, of the differences in the rescheduling solutions provided by the model for the different signalling systems, i.e. ETCS L2 and the conventional fixed-block system. We consider a peak hour in the junction area in which four of the 28 trains enter the area with a delay. We note that initially 29 trains were scheduled within the peak hour, but two trains were delayed such that their entry time moved outside the one-hour window and one train from the hour before was delayed such that its entry time fell within the considered hour.

Table 5. Mean total delay, delay recovery and number of maximum speed profile assignments (speed penalty) of ETCS L2 and conventional fixed-block (original) solutions evaluated in ETCS L2 and original model.

Solution	In ETCS L2			In original	
	Total delay	Delay recovery	Speed penalty	Total delay	Delay recovery
ETCS L2	5186 s	−4.40%	30	6441 s	+22.64%
Original	5582 s	−5.52%	53	5934 s	+0.20%

Table 6. Orders of reordered trains in ETCS L2 and original, i.e. conventional fixed-block, model solutions.

ETCS L2	B $\prec$ A	A $\prec$ C	D $\prec$ A	D $\prec$ C	E $\prec$ F	E $\prec$ H
Original	B $\prec$ A	C $\prec$ A	D $\prec$ A	D $\prec$ C	F $\prec$ E	H $\prec$ E

If reordering and rerouting are applied in combination with retiming, the mean total delays are 5186 s for ETCS L2 and 5934 s for conventional fixed-block signalling, as shown in Table 5. Additionally, Table 5 gives the total delay of the cross-evaluations, i.e. the ETCS L2 solution evaluated in conventional fixed block (6441 s) and the fixed-block solution evaluated in ETCS L2 (5582 s). This instance is the one with the highest impact of the ETCS L2 optimisation, showing a 7.09% reduction in objective values in ETCS L2 over conventional fixed block when both evaluated in ETCS L2. For completeness, Table 5 also reports the mean delay recovery and the number of times that the model assigns a maximum speed profile to a train. Note that the delay recovery is negative for the conventional fixed-block and ETCS L2 solutions evaluated in ETCS L2. This indicates that the total exit delay exceeds the total entry delay. As Table 5 shows, this different distribution of the delay does not go at the expense of the overall total delay.

In the following, we focus on a subset of nine trains (A to I) that share a part of their route in the timetable and/or in the rescheduling solutions with train E, which is crucial for the difference between the fixed-block and the ETCS L2 solutions. Trains A to H are labelled alphabetically according to their original scheduled order, while Train I is scheduled to run on a parallel track. Figure 6 illustrates the blocking times of the trains along the route of train E, which is indicated in Figure 5(a).

Within this subset, trains A and C suffer entry delays of 826 and 466 s, respectively. Figure 6(a,b) illustrate the optimised ETCS L2 and fixed-block solutions by a schematic representation of their blocking times in terms of the TDSs along train E's route. Table 6 details the train ordering decisions for ETCS L2 and fixed block, listing only the train pairs that are reordered.

The ETCS L2 solution includes three reordering decisions and one rerouting decision with respect to the timetable: B goes before A, D goes before A and C, and D is partially rerouted. The reorderings of A and C with B and D directly follow from them being delayed upon entry, letting B and D run according to schedule. The rerouting of D, which in the timetable only shares the entry and exit blocks with E, frees up some space on the fully packed parallel track. Table 7 presents the entry and exit delays of the trains. Note that only the trains with a positive total delay are included.

The original solution for conventional fixed-block includes the same rescheduling decisions as the ETCS L2 solution. Additionally, A and C are mutually reordered and E is reordered with F and H. Further delaying E allows F and H to run without delays. Actually,

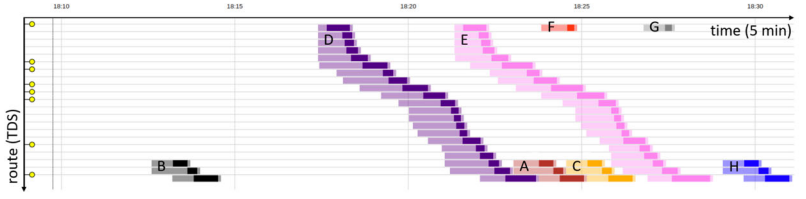

(a) Schematic blocking time diagram of ETCS L2 solution.

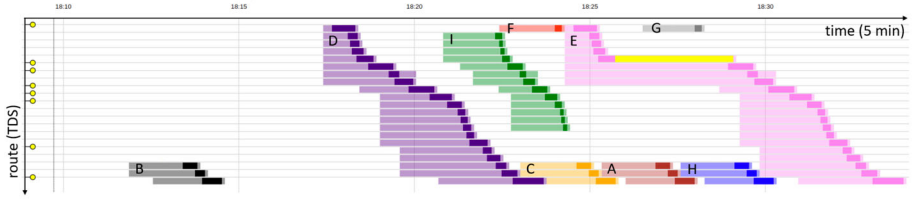

(b) Schematic blocking time diagram of conventional fixed-block solution.

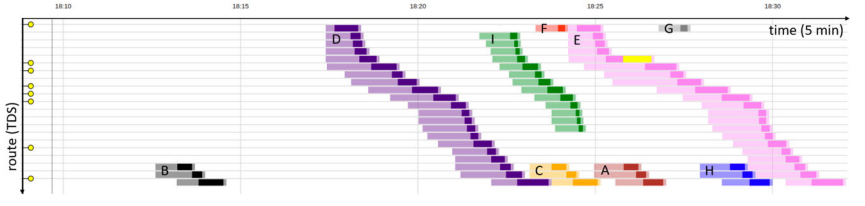

(c) Schematic blocking time diagram of conventional fixed-block in ETCS L2 evaluation.

Figure 6. Schematic blocking time diagrams of rescheduling solutions along train E's route in terms of TDSs, aligned in time. Physical occupation times and additional delays are indicated by dark colours and yellow, respectively. (a) Schematic blocking time diagram of ETCS L2 solution. (b) Schematic blocking time diagram of conventional fixed-block solution and (c) Schematic blocking time diagram of conventional fixed-block in ETCS L2 evaluation.

Table 7. Entry and exit delays of trains with positive total delay in the listed solution evaluations (original is conventional fixed-block). The imposed entry delay is indicated in the heading.

Delays (s)	**Train A** (+826)		**Train C** (+466)		**Train E** (+0)		**Train I** (+0)		**Total**
	Entry	Exit	Entry	Exit	Entry	Exit	Entry	Exit	
ETCS L2	826	813	524	537	0	0	48	59	2807
Original	996	988	466	493	177	314	5	0	3439
Original in ETCS L2	965	924	466	453	174	197	0	0	3179

the two trains are running ahead of schedule to minimise the delay of train E. The reordering of E and F allows for the rerouting of I away from the same parallel track D was rerouted from.

Figure 6(c) shows the schematic blocking time diagram of the cross-evaluation: we apply the ordering and routing decisions of the conventional fixed-block solution considering ETCS L2 signalling. Table 7 provides an overview of the entry and exit delays of the trains under 'Fixed block in ETCS L2'. we take a step back to the overall delays presented in Table 5 for the overall picture. Comparing the total delay obtained by evaluating the conventional fixed-block solution in ETCS L2 with the total delay obtained by the ETCS L2 solution (in ETCS L2), indicates an additional delay of 396 s due to the different rescheduling decisions. Comparing the total delay of the fixed-block in ETCS L2 evaluation and of the conventional

fixed-block solution (in fixed-block), indicates a saving of 352 s delay due to the ETCS L2 blocking times. We note that solutions are more sensitive to the signalling system (the model) than to the rescheduling decisions.

For this case study instance, we conclude that due to the significant difference in blocking times under ETCS L2 and conventional fixed block signalling, the conventional fixed-block solution contains additional rescheduling decisions that lead to a worse performance in ETCS L2. From an operational perspective it is therefore relevant to incorporate DTG principles into CDR model for a more accurate assessment of the performance of CDR under DTG.

5.5. Real-time applicability

In this section, we discuss the computational performance of the RECIFE-MILP model ehanced fro ETCS L2. Given the real-time nature of the CDR problem, we specifically include the real-time applicability in this discussion. Also, we compare the computational performance of the ETCS L2 with the original RECIFE-MILP model for conventional fixed-block signalling.

With a computation time limit of 3600 s, 92% of the junction scenarios and 99% of the corridor scenarios are solved to optimality. The remaining scenarios are solved sub-optimally, with mean optimality gaps of 0.28% and 0.43% for the junction and corridor case study, respectively. In line with these numbers, the time to reach optimality is often far from 3600 s, overall averaging 475 s for the junction case study and 233 s for the corridor case study. The variation in the utilised computation time is illustrated by Figure 7, which plots the percentage of scenarios solved to optimality over the computation time. Indeed, the curve's decreasingly increasing nature highlights the relative high likelihood of short utilised computation times.

In Figure 7, the practical computation times of 180 and 300 s are highlighted. For the respective case studies, 13% and 56% of the scenarios are optimally solved within 180 s, and 54% and 68% within 300 s. This shows that the model can perform in real-time.

The model's real-time performance is further discussed based on the additional computational results given in Table 8, which include the absolute and relative optimality gaps after 180 and 300 s. For the absolute and relative optimality gap, the real-time solution is compared with the real-time lower bound and the lower bound after 3600 s(so in most cases of the optimal solution), respectively. As suggested by the differences between the relative and the absolute optimality gap, it is primarily the lower bound that is improved in the further optimisation process. The relative optimality gaps indeed support the real-time applicability of the model, with all mean values below 0.5%, despite occasional maximum relative optimality gaps over 20%.

Next to the computational results for the ETCS L2 model, Table 8 reports some results for the original RECIFE-MILP model. The original model outperforms the ETCS L2 model in nearly all listed aspects, as can be expected from the different model dimensions reported in Table 2. Only the mean optimality gap of the sub-optimal solutions at 3600 s are in favour of the ETCS L2 model. As this only includes one optimality gap on the side of the original model, we cannot take the number as a representative. A notable result of the original model is the clean score for the corridor case study; already optimally solving all scenarios

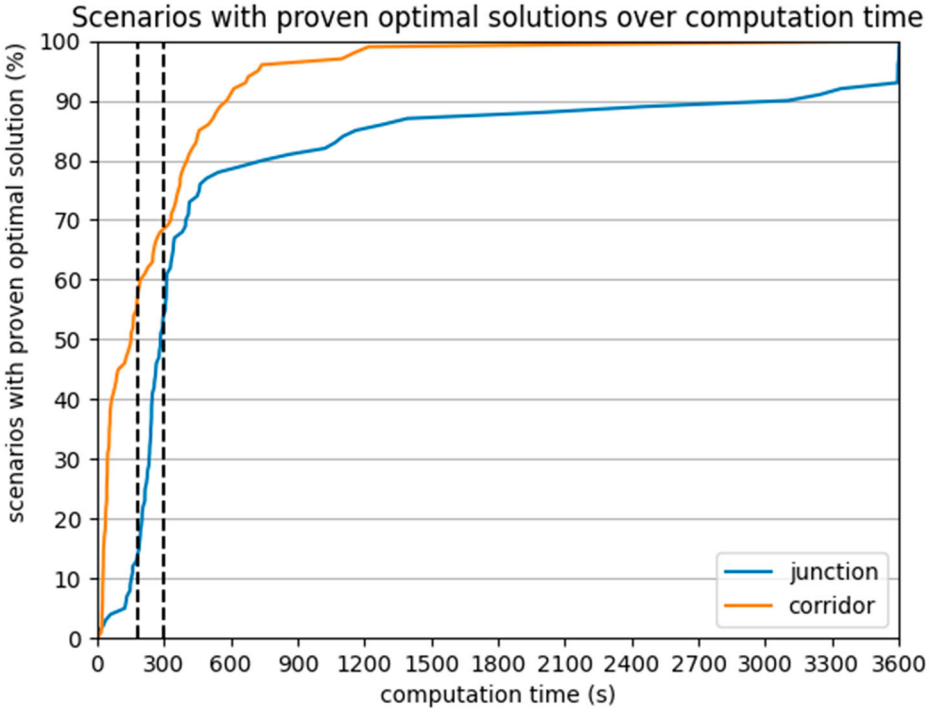

Figure 7. Percentage of scenarios with a proven optimal solution over computation time. The dashed vertical lines correspond to practical computation times of 180 and 300 s.

Table 8. Computational performance results for the ETCS L2 and original RECIFE-MILP model.

	ETCS L2 model		Original model	
	Junction	Corridor	Junction	Corridor
Mean computation time	475 s	233 s	334 s	25 s
Mean optimality gap of sub-opt solutions	0.28%	0.43%	2.62%	0.00%
% scenarios with proven optimal solution				
- in 180 s	13%	56%	57%	100%
- in 300 s	54%	68%	73%	100%
- in 3600 s	92%	99%	92%	100%
Absolute optimality gap				
- at 180 s(mean)	1.38%	1.45%	–	0%
- at 180 s(max)	8.07%	21.76%	–	0%
- at 300 s(mean)	0.53%	0.88%	–	0%
- in 300 s(max)	4.24%	20.95%	–	0%
Relative optimality gap				
- at 180 s(mean)	0.41%	0.01%	–	0%
- at 180 s(max)	2.57%	15.89%	–	0%
- at 300 s(mean)	0.23%	0.01%	–	0%
- in 300 s(max)	2.57%	0.43%	–	0%

within 180 s. To a smaller extent, it also holds for the ETCS L2 model that the corridor area is faster to solve than junction.

Despite being outperformed by the original model, the ETCS L2 model demonstrates robust real-time performance by solving a significant portion of the scenarios to optimality within practical time limits and maintaining minimal optimality gaps for sub-optimally

solved scenarios. Thus, the ETCS L2 model shows promise for real-time applications, providing a good balance between computational efficiency and solution quality. We note that the real-time applicability can be improved with a more effective model formulation and solution algorithm.

6. Conclusions

In this paper, we assessed the operational relevance of modelling conflict detection and resolution (CDR) for distance-to-go (DTG) railway signalling. CDR models originally developed for conventional fixed-block signalling can be adapted to DTG signalling by incorporating train- and speed-dependent brake indication points and blocking times to capture the braking curve supervision in DTG signalling. By integrating the DTG modelling approach into the state-of-the-art RECIFE-MILP model, we obtain a CDR model for operations under the European Train Control System Level 2 with Trackside Train Detection (ETCS L2). Application to two real-world case studies, a complex junction with dense mixed traffic and a corridor with regular mixed traffic, shows longer computation times to obtain (near-)optimal solutions under delay scenarios compared to conventional fixed-bock signalling, while maintaining acceptable real-time performance of the enhanced model.

The underlying signalling system causes the CDR model to obtain different rescheduling decisions and total train delay. The ETCS L2 model outperformed the original model with respect to the minimised total train delay. While the overall reduction in delay under ETCS L2 compared to the conventional fixed-block signalling is limited, several case study instances showed significant reductions of up to 7%. Most of the reductions are directly attributable to the shorter, train- and speed-dependent train separation enabled by ETCS L2 signalling, while additional reductions arise from different rescheduling decisions, indirectly benefiting from the DTG principles. Furthermore, the inclusion of a penalty for using maximum speed profiles in the enhanced model objective results in trains running less frequently with the maximum speed profile. This provides a secondary benefit in terms of energy consumption.

Future research is needed to investigate the possibility of using the model for other DTG signalling systems such as the ETCS Level 2 with onboard train position and train integrity monitoring systems of ETCS Level 2 Virtual Block and ETCS Level 2 Moving Block. The modelling of ETCS Level 2 Virtual Block requires a track discretisation finer than trackside train detection sections, and such finer discretisation can also be used to approximate ETCS Level 2 Moving Block. Other topics to be investigated are the incorporation of additional and/or more advanced speed profile options, as well as the performance of the model in real-time and within a framework including a simulation environment enabling simulation-based validation. Future work should also assess the model's robustness against stochastic factors beyond entry delay that can occur in real-world settings, e.g. dwell times or braking distances. Finally, a valuable extension would be to analyse the trade-off between total delay and the assignment of maximum speed profiles.

Overall, the research topic needs to be further investigated to produce more and more efficient algorithms to enable the use of decision support systems for optimised real-time traffic management which also consider DTG signalling constraints. This includes the fine-tuning of (existing) model formulations and implementations. Promising in terms of computational performance are (geographical) decomposition approaches.

To conclude, the key takeaways from this paper are as follows. First, by incorporating train- and speed-dependent brake indication points and blocking times, existing CDR models can be enhanced to be applicable to DTG signalling. Second, integrating DTG principles into CDR models can lead to different rescheduling decisions and a reduction in total train delay. Third, although further improvements in computational efficiency are recommended, the computation performance of the presented CDR model for DTG is acceptable for real-time application.

Disclosure statement

No potential conflict of interest was reported by the author(s).

Funding

This research has received funding from the Shift2Rail Joint Undertaking (JU) under grant agreement No. 101015416 (PERFORMINGRAIL). The JU receives support from the European Union's Horizon 2020 research and innovation programme and the Shift2Rail JU members other than the Union.

ORCID

Nina D. Versluis http://orcid.org/0009-0006-5368-8912
Paola Pellegrini https://orcid.org/0000-0002-6087-651X
Egidio Quaglietta https://orcid.org/0000-0002-7936-5832
Rob M.P. Goverde https://orcid.org/0000-0001-8840-4488
Joaquin Rodriguez https://orcid.org/0000-0002-5674-2439

References

Bazaraa , M. S., J. J. Jarvis, and H. D. Sherali. 2008. *Linear Programming and Network Flows*. Hoboken, New Jersey: John Wiley & Sons.

Bettinelli, A., A. Santini, and D. Vigo. 2017. "A Real-Time Conflict Solution Algorithm for the Train Rescheduling Problem." *Transportation Research Part B: Methodological* 106:237–265. https://doi.org/10.1016/j.trb.2017.10.005.

Brünger, O., and E. Dahlhaus. 2014. "Running Time Estimation." In *Railway Timetabling and Operations: Analysis, Modelling, Optimisation, Simulation, Performance, Evaluation*, edited by I. Hansen and J. Pachl, 65–89. Hamburg, Germany: Eurailpress.

Cacchiani, V., D. Huisman, M. Kidd, L. Kroon, P. Toth, L. Veelenturf, and J. Wagenaar. 2014. "An Overview of Recovery Models and Algorithms for Real-Time Railway Rescheduling." *Transportation Research Part B: Methodological* 63:15–37. https://doi.org/10.1016/j.trb.2014.01.009.

Caimi, G., M. Fuchsberger, M. Laumanns, and M. Lüthi. 2012. "A Model Predictive Control Approach for Discrete-Time Rescheduling in Complex Central Railway Station Areas." *Computers & Operations Research* 39 (11): 2578–2593. https://doi.org/10.1016/j.cor.2012.01.003.

Corman, F., A. D'Ariano, D. Pacciarelli, and M. Pranzo. 2009. "Evaluation of Green Wave Policy in Real-Time Railway Traffic Management." *Transportation Research Part C: Emerging Technologies* 17 (6): 607–616. https://doi.org/10.1016/j.trc.2009.04.001.

D'Ariano, A., F. Corman, D. Pacciarelli, and M. Pranzo. 2008. "Reordering and Local Rerouting Strategies to Manage Train Traffic in Real-Time." *Transportation Science* 42 (4): 405–419. https://doi.org/10.1287/trsc.1080.0247.

D'Ariano, A., D. Pacciarelli, and M. Pranzo. 2007. "A Branch and Bound Algorithm for Scheduling Trains in a Railway Network." *European Journal of Operational Research* 183 (2): 643–657. https://doi.org/10.1016/j.ejor.2006.10.034.

D'Ariano, A., M. Pranzo, and I. A. Hansen. 2007. "Conflict Resolution and Train Speed Coordination for Solving Real-Time Timetable Perturbations." *IEEE Transactions on Intelligent Transportation Systems* 8 (2): 208–222. https://doi.org/10.1109/TITS.2006.888605.

Davis, W. J. 1926. "The Tractive Resistance of Electric Locomotives and Cars." *General Electric Review* 29: 685–707.
ERA-UNISIG-EEIG ERTMS Users Group. 2016. *ERTMS/ETCS System Requirements Specification (Subset-026)*.
European Rail Supply Industry Association. 2022. "ERTMS." https://www.ertms.net/.
European Railway Agency. 2020. *Introduction to ETCS Braking Curves*.
Hansen, I. A., and J. Pachl (Editors). 2014. *Railway Timetabling & Operations: Analysis, Modelling, Optimisation, Simulation, Performance Evaluation*. Hamburg, Germany: Eurailpress.
Janssens, M. L. 2022. "Multi Machine Approaches for Conflict Resolution under Moving Block Signalling." Master Thesis, Delft University of Technology, The Netherlands.
Lamorgese, L., and C. Mannino. 2015. "An Exact Decomposition Approach for the Real-Time Train Dispatching Problem." *Operations Research* 63 (1): 48–64. https://doi.org/10.1287/opre.2014.1327.
Lamorgese, L., C. Mannino, D. Pacciarelli, and J. Törnquist Krasemann. 2018. "Train Dispatching." In *Handbook of Optimization in the Railway Industry*, edited by R. Borndörfer, T. Klug, L. Lamorgese, C. Maninno, M. Reuther, and T. Schlechte, 265–283. Cham, Switzerland: Springer.
Leutwiler, F., and F. Corman. 2022. "A Logic-Based Benders Decomposition for Microscopic Railway Timetable Planning." *European Journal of Operational Research* 303 (2): 525–540. https://doi.org/10.1016/j.ejor.2022.02.043.
Leutwiler, F., and F. Corman. 2023. "A Review of Principles and Methods to Decompose Largescale Railway Scheduling Problems." *EURO Journal on Transportation and Logistics* 12:1–17. https://doi.org/10.1016/j.ejtl.2023.100107.
Lippes, S. J. H. 2024. "Distributed Rail Traffic Management under Moving-Block Signalling." Master Thesis, Delft University of Technology, The Netherlands.
Luan, X., Y. Wang, B. De Schutter, L. Meng, G. Lodewijks, and F. Corman. 2018. "Integration of Real-Time Traffic Management and Train Control for Rail Networks – Part 1: Optimization Problems and Solution Approaches." *Transportation Research Part B: Methodological* 115:41–71. https://doi.org/10.1016/j.trb.2018.06.006.
Lusby, R. M., J. Larsen, M. Ehrgott, and D. M. Ryan. 2013. "A Set Packing Inspired Method for Real-Time Junction Train Routing." *Computers & Operations Research* 40 (3): 713–724. https://doi.org/10.1016/j.cor.2011.12.004.
Mannino, C. 2011. "Real-Time Traffic Control in Railway Systems." In *11th Symposium on Algorithmic Approaches for Transportation Modelling, Optimization, and Systems (ATMOS 2011)*, Schloss Dagstuhl-Leibniz-Zentrum für Informatik.
Mannino, C., and A. Mascis. 2009. "Optimal Real-Time Traffic Control in Metro Stations." *Operations Research* 57 (4): 1026–1039. https://doi.org/10.1287/opre.1080.0642.
Marcelli, E., and P. Pellegrini. 2021. "Literature Review toward Decentralized Railway Traffic Management." *IEEE Intelligent Transportation Systems Magazine* 13:234–252. https://doi.org/10.1109/MITS.2020.2970180.
Marcis, A., and D. Pacciarelli. 2007. "Job-Shop Scheduling with Blocking and No-Wait Constraints." *European Journal of Operational Research* 143 (3): 498–517.
Mazzarello, M., and E. Ottiviani. 2007. "A Traffic Management System for Real-Time Traffic Optimisation in Railways." *Transportation Research Part B: Methodological* 41 (2): 246–274. https://doi.org/10.1016/j.trb.2006.02.005.
Pellegrini, P., G. Marlière, R. Pesenti, and J. Rodriguez. 2015. "RECIFE-MILP: An Effective MILP-Based Heuristic for the Real-Time Railway Traffic Management Problem." *IEEE Transactions on Intelligent Transportation Systems* 16 (5): 2609–2619. https://doi.org/10.1109/TITS.2015.2414294.
Pellegrini, P., G. Marlière, and J. Rodriguez. 2014. "Optimal Train Routing and Scheduling for Managing Traffic Perturbations in Complex Junctions." *Transportation Research Part B: Methodological* 59:58–80. https://doi.org/10.1016/j.trb.2013.10.013.
Pellegrini, P., G. Marlière, and J. Rodriguez. 2016. "A Detailed Analysis of the Actual Impact of Real-Time Railway Traffic Management Optimization." *Journal of Rail Transport Planning and Management* 6 (1): 13–31. https://doi.org/10.1016/j.jrtpm.2016.01.002.

Pellegrini, P., R. Pesenti, and J. Rodriguez. 2019. "Efficient Train re-routing and Rescheduling: Valid Inequalities and Reformulation of RECIFE-MILP." *Transportation Research Part B: Methodological* 120: 33–48. https://doi.org/10.1016/j.trb.2018.12.008.

PERFORMINGRAIL. 2022. *Deliverable D4.1: Real-Time Traffic Rescheduling Algorithms for Perturbation Management and Hazard Prevention in Moving-Block Operations*.

Pochet, J., S. Baro, and G. Sandou. 2016. "Supervision and Rescheduling of a Mixed CBTC Traffic on a Suburban Railway Line." In *2016 IEEE International Conference on Intelligent Rail Transportation (ICIRT)*.

Quaglietta, E., P. Pellegrini, R. M. P. Goverde, T. Albrecht, B. Jaekel, G. Marlière, J. Rodriguez, et al. 2016. "The ON-TIME Real-Time Railway Traffic Management Framework: A Proof-of-concept Using a Scalable Standardised Data Communication Architecture." *Transportation Research Part C: Emerging Technologies* 63:23–50. https://doi.org/10.1016/j.trc.2015.11.014.

Reynolds, E., M. Ehrgott, S. J. Maher, A. Patman, and J. Y. T. Wang. 2020. "A Multicommodity Flow Model for Rerouting and Retiming Trains in Real-Time to Reduce Reactionary Delay in Complex Station Areas." *Optimization Online*. https://optimization-online.org/?p = 16475.

Reynolds, E., and S. J. Maher. 2022. "A Data-Driven, Variable-Speed Model for the Train Timetable Rescheduling Problem." *Computers and Operation Research* 142: 105719. https://doi.org/10.1016/j.cor.2022.105719.

Törnquist, J., and J. Persson. 2007. "N-tracked Railway Traffic re-scheduling during Disturbances." *Transportation Research Part B: Methodological* 41 (3): 342–362. https://doi.org/10.1016/j.trb.2006.06.001.

Van den Akker, J. M., C. A. Hurkens, and M. W. Savelsbergh. 2000. "Time-Indexed Formulations for Machine Scheduling Problems: Column Generation." *INFORMS Journal on Computing* 12 (2): 111–124. https://doi.org/10.1287/ijoc.12.2.111.11896.

Versluis, N. D., E. Quaglietta, R. M. P. Goverde, P. Pellegrini, and J. Rodriguez. 2024. "Real-Time Railway Traffic Management under Moving-Block Signalling: A Literature Review and Research Agenda." *Transportation Research Part C: Emerging Technologies* 158: 104438. https://doi.org/10.1016/j.trc.2023.104438.

Xu, P., F. Corman, Q. Peng, and X. Luan. 2017. "A Train Rescheduling Model Integrating Speed Management during Disruptions of High-Speed Traffic under a Quasi-moving Block System." *Transportation Research Part B: Methodological* 104:638–666. https://doi.org/10.1016/j.trb.2017.05.008.

Yi, X., G. Marlière, P. Pellegrini, J. Rodriguez, and R. Pesenti. 2023. "Coordinated Train Rerouting and Rescheduling in Large Infrastructures." *Transportation Research Procedia* 72:319–326. https://doi.org/10.1016/j.trpro.2023.11.410.

Zhan, S., S. C. Wong, P. Shang, and S. M. Lo. 2022. "Train Rescheduling in a Major Disruption on a High-Speed Railway Network with Seat Reservation." *Transportmetrica A: Transport Science* 18 (3): 532–567. https://doi.org/10.1080/23249935.2021.1877369.

Zhang, S., Y. Cheng, K. Chen, C. Ma, J. Wei, and X. Hu. 2024. "A General Metro Timetable Rescheduling Approach for the Minimisation of the Capacity Loss after Random Line Disruption." *Transportmetrica A: Transport Science* 20 (3): 2204965. https://doi.org/10.1080/23249935.2023.2204965.

Appendix. Overview of sets, parameters and variables

Table A1. Sets, parameters and variables in the MILP model formulation, with new and updated elements in **bold**.

Symbol	Description
Sets	
T	set of trains
R	set of routes
$R_t \subset R$	set of routes available to train $t \in T$
L	set of locations
$L_t \subset L$	set of locations which can be used by train $t \in T$
$L^r \subset L$	set of locations along route $r \in R$
$OL_{t,r,l} \subset L^r$	set of locations along route $r \in R_t$ such that if train $t \in T$ starts occupying it, the train has not yet cleared location $l \in L^r$, $l \notin OL_{t,r,l}$
S	set of stations
$S_t \subset S$	set of stations where train $t \in T$ has a scheduled stop
$L_{t,s} \subset L_t$	set of locations that can be used by train $t \in T$ for stopping at station $s \in S_t$
$\hat{L}_{t,t',l} \subset L$	set of locations $l' \in L_t \cap L_{t'}$ which may be used by trains $t, t' \in T$ such that if t precedes t' on l, then t precedes t' on l'
$\mathbf{P} \subset \boldsymbol{L}$	set of speed assignment locations
$\mathbf{P^r} \subset \mathbf{P}$	set of speed assignment locations along route $r \in R$
Parameters	
$\pi_{r,l}, \sigma_{r,l} \in L^r$	preceding location and succeeding location of location $l \in L^r$ along route $r \in R$
$\boldsymbol{\rho_{r,l} \in \mathbf{P^r}}$	speed assignment location associated with location $l \in L^r$ along route $r \in R$
$s_l \in \{0, 1\}$	$= 1$ if location $l \in L$ lies in a switch area
$l_\infty \in L$	dummy location considered as destination for all trains
$init_t \in \mathbb{R}_+$	earliest time at which train $t \in T$ can be operated
$sched_t \in \mathbb{R}_+$	scheduled arrival time of train $t \in T$ at dummy destination location $l_\infty \in L$
$dw_{t,s} \in \mathbb{R}_+$	minimum dwell time for train $t \in T$ at station $s \in S_t$
$a_{t,s}, d_{t,s} \in \mathbb{R}_+$	scheduled arrival/departure time for train $t \in T$ at station $s \in S_t$
$for_{r,l} \in \mathbb{R}_+$	formation time, i.e. setup and reaction time, of location $l \in L^r$ along route $r \in R$
$rel_{r,l} \in \mathbb{R}_+$	release time of location $l \in L^r$ along route $r \in R$
$rt_{t,r,l} \in \mathbb{R}_+$	minimum running time for train $t \in T$ from location $l \in L_t$ to $\sigma_{r,l}$ along route $r \in R_t$
$\boldsymbol{\Delta rt_{t,r,l} \in \mathbb{R}_+}$	additional running time for train $t \in T$ from location $l \in L_t$ to $\sigma_{r,l}$ along route $r \in R_t$ in case of scheduled speed profile
$ct_{t,r,l} \in \mathbb{R}_+$	minimum clearing time for train $t \in T$ of location $l \in L_t$ along route $r \in R_t$
$\boldsymbol{\Delta ct_{t,r,l} \in \mathbb{R}_+}$	additional clearing time for train $t \in T$ of location $l \in L_t$ along route $r \in R_t$ in case of scheduled speed profile
$\boldsymbol{ref^s_{t,r,l} \in L^r}$	reference brake location for location $l \in L^r$ along route $r \in R_t$ for train $t \in T$ approaching according to scheduled speed profile
$\boldsymbol{ref^m_{t,r,l} \in L^r}$	reference brake location for location $l \in L^r$ along route $r \in R_t$ for train $t \in T$ approaching according to maximum speed profile
$\boldsymbol{lag^s_{t,r,l} \in \mathbb{R}_+}$	time by which blocking of location $l \in L^r$ by train $t \in T$ running according to scheduled speed profile along route $r \in R_t$ can be postponed after passing $ref^s_{t,r,l}$
$\boldsymbol{lag^m_{t,r,l} \in \mathbb{R}_+}$	time by which blocking of location $l \in L^r$ by train $t \in T$ running according to maximum speed profile along route $r \in R_t$ can be postponed after passing $ref^m_{t,r,l}$
$M \in \mathbb{R}_+$	a large constant
$w_t \in \mathbb{R}_+$	train priority weights for objective function
$\boldsymbol{w \in \mathbb{R}_+}$	maximum speed profile penalty
Variables	
$y_{t,t',l} \in \{0, 1\}$	$= 1$ if train $t \in T$ blocks location $l \in L_t \cap L_{t'}$ before train $t' \in T$
$x_{t,r} \in \{0, 1\}$	$= 1$ if train $t \in T$ uses route $r \in R_t$
$\boldsymbol{v^s_{t,r,l} \in \{0, 1\}}$	$= 1$ if train $t \in T$ passes speed assignment location $l \in \mathrm{P}^r$ along route $r \in R_t$ according to scheduled speed profile
$\boldsymbol{v^m_{t,r,l} \in \{0, 1\}}$	$= 1$ if train $t \in T$ passes speed assignment location $l \in \mathrm{P}^r$ along route $r \in R_t$ according to maximum speed profile
$o_{t,r,l} \in \mathbb{R}_+$	occupation starting time of train $t \in T$ on location $l \in L^r$ along route $r \in R_t$
$o^+_{t,r,l} \in \mathbb{R}_+$	extended occupation time of train $t \in T$ between locations $l \in L^r$ and $\sigma_{r,l} \in L^r$ along route $r \in R_t$
$b^s_{t,l}, b^e_{t,l} \in \mathbb{R}_+$	time at which train $t \in T$ starts/ends blocking location $l \in L_t$
$z_t \in \mathbb{R}_+$	delay suffered by train $t \in T$ when exiting the infrastructure and/or arriving at destination
$z_{t,s} \in \mathbb{R}_+$	delay suffered by train $t \in T$ when stopping at station $s \in S_t$